



Evaluation of Lift Formulas Applied to Low-Reynolds-Number Unsteady Flows

Shizhao Wang,* Xing Zhang,[†] and Guowei He[‡]

Chinese Academy of Sciences, 100190 Beijing, People's Republic of China

and

Tianshu Liu[§]

Western Michigan University, Kalamazoo, Michigan 49008

DOI: 10.2514/1.J053042

Different lift decompositions into the elemental terms are compared based on direct numerical simulations of a flapping flat plate and a flapping rectangular wing at low-Reynolds-number flows. The simple lift formula is given as a useful approximate form that has the vortex force and local acceleration terms. The accuracy of the simple lift formula in lift estimation is quantitatively evaluated in comparison with the general force formulas based on the fully resolved two- and three-dimensional unsteady velocity fields and the planar velocity fields at several spanwise locations in simulated particle-image-velocimetry measurements. In addition, the mathematical connections between the different force formulas are discussed.

Nomenclatures

A	= heaving amplitude, m
AR	= wing aspect ratio
Cl	= lift coefficient
c	= wing chord, m
F	= aerodynamic force, N
F_z	= lift, N
f	= flapping frequency, s^{-1}
\mathbf{l}	= Lamb vector, $m \cdot s^{-2}$
p	= pressure, Pa
Q	= second invariant of velocity gradient tensor, s^{-2}
q	= dynamic pressure, Pa
Re	= Reynolds number
S	= wing area, m^2
St	= flapping Strouhal number
T	= flapping period, s
t	= time, s
U_∞	= freestream velocity, $m \cdot s^{-1}$
\mathbf{u}	= fluid velocity, $m \cdot s^{-1}$
V_f	= control volume
\mathbf{x}	= position vector, m
z_c	= vertical position of the wing center, m
α	= angle of attack, deg
Σ	= outer surface of a control volume surrounding a body
τ	= viscous stress tensor, $N \cdot m^{-2}$
ω	= vorticity, s^{-1}

I. Introduction

THE connection between the generation of aerodynamic lift and flow structures has been a key topic in the development of

Received 4 September 2013; revision received 11 January 2014; accepted for publication 3 March 2014; published online 7 August 2014. Copyright © 2014 by the American Institute of Aeronautics and Astronautics, Inc. All rights reserved. Copies of this paper may be made for personal or internal use, on condition that the copier pay the \$10.00 per-copy fee to the Copyright Clearance Center, Inc., 222 Rosewood Drive, Danvers, MA 01923; include the code 1533-385X/14 and \$10.00 in correspondence with the CCC.

*Assistant Professor, State Key Laboratory of Nonlinear Mechanics, Institute of Mechanics.

[†]Associate Professor, State Key Laboratory of Nonlinear Mechanics, Institute of Mechanics.

[‡]Professor, State Key Laboratory of Nonlinear Mechanics, Institute of Mechanics; hgw@lnm.imech.ac.cn (Corresponding Author).

[§]Professor, Department of Mechanical and Aerospace Engineering. Senior Member AIAA.

aerodynamics models. Recently, this problem has attracted more focused attention due to its relevance to low-Reynolds-number flapping flight associated with micro air vehicles [1,2]. To understand the physical mechanisms of flapping flight, it is required to estimate the aerodynamic lift from unsteady velocity fields obtained by computational-fluid-dynamics codes and particle-image-velocimetry (PIV) measurements in wind tunnels [3–10]. The Kutta-Joukowski (K-J) theorem is probably the earliest and simplest expression directly relating aerodynamic lift to velocity-related quantities. The K-J theorem has been incorporated in vortex-based aerodynamics models for low-Reynolds-number flapping flight [11–15]. In addition, the K-J theorem has been widely used in existing studies to infer the lift after the circulation is estimated by integrating the vorticity field in a selected cross-section region near wings or in wakes generated in flapping flight. However, lift estimation using the K-J theorem based on PIV measurements in the wakes of slowly flying birds gave a significantly lower value of the lift that cannot support the bird weight [5,7]. The K-J theorem as a quasi-steady model cannot correctly capture the waveform and phase of the instantaneous lift in highly unsteady flows at low Reynolds numbers in flapping flight.

The general force expressions have been extensively discussed by Saffman [16] in the framework of inviscid flows. From the Navier-Stokes (NS) equations, various force expressions have been derived depending on how to transform the pressure term to the velocity-related quantities [17–25]. In particular, Noca et al. [22] gave the force expressions called “impulse equation”, “momentum equation”, and “flux equation”. Wu et al. [24] derived the force expressions by using “derivative-moment transformations”. By introducing an auxiliary velocity potential satisfying suitable boundary conditions and projecting the NS equations on the gradient of the potential, Quartapelle and Napolitano [18], Howe [19], and Chang [20] were able to extract the explicit pressure force from the pressure term and decompose the force into several terms whose physical meanings become clear. In principle, a general lift formula can be derived by directly projecting these general force expressions onto the direction normal to the incoming flow. Many terms appear as a consequence of eliminating the troublesome pressure term, and thus a concise form of the lift expressions cannot be obtained in such a way. Furthermore, the physical meanings of some terms in these lift expressions cannot be easily elucidated, and their relative contributions to the lift cannot be clearly distinguished.

Although various lift decompositions into the elemental terms are equivalent, from a standpoint of application, good lift decomposition should have a minimal number of terms with lucid physical meanings such that the flow structures responsible for lift generation can be clearly identified. Recently, it is recognized that the troublesome

pressure term can be neglected in the first-order approximation when a sufficiently large rectangular control domain is considered. In this case, the lift can be expressed by only the two main terms: the Lamb vector integral for the vortex lift and the local fluid acceleration for the unsteady inertial effect [26]. Because a rectangular control domain is usually used in applications, this lift formula is generally applicable to unsteady separated flows associated with forward flapping flight. The advantage of this lift formula is that it is very simple but sufficiently accurate, and the terms have clear physical meanings. For convenience of expression, it is referred to as the simple lift formula in this paper. For a completely inviscid flow, the simple lift formula is reduced to that given by Saffman [16].

The objective of this work is to evaluate the simple lift formula in comparison with the general force formulas given by Noca et al. [22] and Wu et al. [24] based on direct numerical simulations (DNSs) of a flapping flat-plate airfoil and a flapping rectangular wing. An emphasis is placed on identification of the dominant terms in these formulas and clarification of the physical meanings of these terms. Although the simple lift formula is approximate, unlike the accurate force formulas given by Noca et al. [22] and Wu et al. [24], it is useful particularly in processing experimental and numerical velocity data. This paper is organized as follows. The simple lift formula and the general force formulas of Noca et al. [22] and Wu et al. [24] are described. The numerical method, the immersed boundary method based on discrete stream function formulation, is briefly described. Then, flows over a flapping flat plate and a flapping rectangular wing are simulated. The lift coefficients obtained by using the simple lift formula are compared with those given by Noca et al. [22] and Wu et al. [24]. In particular, the contributions of all the terms in these formulas are evaluated such that the dominant terms can be identified. It is found that the simple lift formula with only two dominant terms is able to predict with a good accuracy the unsteady lift in complex flows. In addition, the mathematical connections between the different force formulas are discussed in Appendix A. The dominant terms contributing to the drag coefficient in the different force formulas are also identified in Appendix B.

II. Lift Formulas

The general force expressions have been derived from the NS equations in [17–25]. Here, the simple lift formula and the typical lift formulas given by Noca et al. [22] and Wu et al. [24] are summarized. In Appendix A, the mathematical connections between the different force formulas given by Noca et al. [22], Wu et al. [24], and Chang [20] are discussed.

A. Simple Lift Formula

The force acting on a body immersed in a fluid flow is usually calculated by

$$\begin{aligned} \mathbf{F} &= -\oint_{\partial B} (-p\mathbf{I} + \boldsymbol{\tau}) \cdot \mathbf{n} dS \\ &= -\rho \int_{V_f(t)} \frac{D\mathbf{u}}{Dt} dV + \oint_{\Sigma} (-p\mathbf{I} + \boldsymbol{\tau}) \cdot \mathbf{n} dS \end{aligned} \quad (1)$$

where p and $\boldsymbol{\tau}$ are the pressure and viscous stress tensor, respectively, \mathbf{I} is the unit tensor, V_f denotes the control volume of fluid, $dV_f = \partial B + \Sigma$ is the total control surface, ∂B denotes the control surface enclosing the body B , Σ denotes an outer control surface in which the body is enclosed, and \mathbf{n} is the unit normal vector pointing to the outside of a control surface. By using the NS equations and Gauss's theorem, Eq. (1) can be expressed as

$$\begin{aligned} \mathbf{F} &= \underbrace{-\rho \int_{V_f} \frac{\partial \mathbf{u}}{\partial t} dV}_{A} + \underbrace{\rho \int_{V_f} \mathbf{u} \times \boldsymbol{\omega} dV}_{B} - \underbrace{\oint_{\Sigma} p \mathbf{n} dS}_{C} \\ &\quad - \underbrace{\oint_{\Sigma} \rho \frac{q^2}{2} \mathbf{n} dS}_{D} + \underbrace{\oint_{\Sigma} \mathbf{n} \cdot \boldsymbol{\tau} dS}_{E} - \underbrace{\oint_{\partial B} \rho \frac{q^2}{2} \mathbf{n} dS}_{F} \end{aligned} \quad (2)$$

where \mathbf{u} is the velocity, $\boldsymbol{\omega}$ is the vorticity, and $q = |\mathbf{u}|$. The term A in Eq. (2) is a volume integral of the local acceleration of fluid induced by a moving solid body and unsteady flow structures as the unsteady inertial effect. The term B is a volume integral of the Lamb vector $\mathbf{l} = \mathbf{u} \times \boldsymbol{\omega}$ that represents the vortex force. The terms C and D are the surface integral of the total pressure $p + \rho q^2/2$ on the outer control surface Σ , and the term E is the surface shear stress on the outer control surface Σ . The term F is the boundary term related to the motion of body boundary ∂B . In an inviscid irrotational unsteady flow where the terms B , C , D , and E in Eq. (2) vanish, the remaining terms A and F together are interpreted as the added mass force in ideal fluid mechanics. For a thin wing, the term F is small, which is interpreted as the part of the added mass force associated with the fluid virtually occupying the body domain B (a virtual fluid body).

The lift on a body is given by $F_z = \mathbf{k} \cdot \mathbf{F}$, where \mathbf{k} is the unit vector normal to the freestream. A rectangular domain D is selected as a control volume to simplify the lift expression (as shown in Fig. 3). For a sufficiently large boundary Σ , the viscous stress term $\mathbf{k} \cdot (\boldsymbol{\tau} \cdot \mathbf{n})$ on the most portion of Σ is zero except in a wake, and thus the contribution of the term E to the lift can be neglected. The major problem is to estimate the terms $C + D$ in the right-hand side (RHS) of Eq. (2) that is the surface integral of the total pressure $p + \rho q^2/2$ on a fixed rectangular outer control surface Σ . The total pressure is $p + \rho q^2/2 = C(t) - \rho \partial \phi / \partial t$, where ϕ is the velocity potential, and $C(t)$ is an unknown function. Because the unit normal vector \mathbf{n} on the four vertical faces of the rectangular control volume is perpendicular to \mathbf{k} ($\mathbf{k} \cdot \mathbf{n} = 0$), the integral in $C + D$ on the four vertical faces is zero. The remaining part of $C + D$ is contributed by the integral on the top and bottom faces of the rectangular outer control surface, which is $S_0 \rho \partial / \partial t (\langle \phi^+ \rangle_A - \langle \phi^- \rangle_A) - (\langle C^+ \rangle_A - \langle C^- \rangle_A)$, where $\langle \rangle_A$ is the area-averaging operator, S_0 is the area of the top or bottom face that is a constant, and the superscripts + and - denote the values at the top and bottom faces. When the top and bottom faces move sufficiently away from a wing, the value of $\langle \phi^+ \rangle_A - \langle \phi^- \rangle_A$ approaches zero because $\phi \sim |z|^{-n} \rightarrow 0$ as $|z| \rightarrow \infty$, where $|z|$ is the distance of the top or bottom face to the wing, and n is a positive exponent to be determined. The difference $\langle C^+ \rangle_A - \langle C^- \rangle_A$ represents the asymmetry of the far-field flow with respect to the x axis. When the freestream flow is steady, $C(t)$ is constant because $\phi \sim |z|^{-n} \rightarrow 0$ as $|z| \rightarrow \infty$, and therefore $\langle C^+ \rangle_A - \langle C^- \rangle_A = 0$. In normal forward flapping flight, therefore, it is plausible to assume that the total pressure term is small for a sufficiently large rectangular domain. However, the previous argument is qualitative. The values of the total pressure term and the terms E and F in a finite domain should be quantitatively evaluated through DNS for a flapping flat plate and a flapping rectangular wing.

The contribution of the total pressure term has been evaluated quantitatively by Wang et al. [26] through DNS for a stationary and flapping flat plate. In computations, the top and bottom boundaries of a rectangular domain are located at $z/c = \pm 6$, where c is the chord of the plate. The total pressure term fluctuates at the same frequency as the unsteady lift with a certain phase shift, indicating that it is indeed perturbed by the unsteady vortical structures. The relative contribution by the total pressure term to the time-averaged lift is less than 2%. Based on numerical simulations, a rule of thumb is suggested for the size of a selected rectangular control surface to ignore the contribution of the total pressure term. It is suggested that $|z|/(c \sin \alpha) \sim O(10)$ for a stationary plate and $|z|/(2A) \sim O(10)$ for a flapping plate, where $|z|$ is the distance between the top/bottom boundary and the body, c is the chord, α is the angle of attack (AoA), and A is the flapping amplitude. Therefore, when a rectangular control volume is sufficiently large, it is a reasonable approximation to ignore the contribution of the total pressure term in Eq. (2). However, when the rectangular domain in velocity measurements is limited, the contribution of the total pressure term on the outer control surface should be evaluated for accurate lift estimation.

Under the aforementioned approximations, a simple lift formula is given by

$$F_z = \rho \mathbf{k} \cdot \int_{V_f} \mathbf{u} \times \boldsymbol{\omega} dV - \rho \mathbf{k} \cdot \int_{V_f} \frac{\partial \mathbf{u}}{\partial t} dV - \rho \mathbf{k} \cdot \oint_{\partial B} (q^2/2) \mathbf{n} dS + R_m \quad (3)$$

where $(\mathbf{u} \times \boldsymbol{\omega}) \cdot \mathbf{k}$ is the vertical component of the Lamb vector, and $\mathbf{u} \cdot \mathbf{k}$ is the vertical component of the velocity, and R_m is an error term contributed by the remaining terms in Eq. (2). The vortex lift and the terms associated with the fluid acceleration are the main terms in Eq. (3). In an inviscid irrotational flow as a limiting case, the second and third terms together in the RHS of Eq. (3) are reduced to the added-mass force. In fact, the third term is negligibly small for a thin wing, and it is zero for the plat-plate airfoil/wing considered in this paper. As indicated in Appendix A, the term related to the local acceleration $\partial \mathbf{u} / \partial t$ in Eq. (3) can be decomposed into a number of the vorticity-related terms, particularly those associated with $\mathbf{x} \times \partial \boldsymbol{\omega} / \partial t$ and $\mathbf{x} \times \mathbf{n} \times (\mathbf{u} \times \boldsymbol{\omega})$. The apparent advantage of such decomposition is that the volume integrals of the vorticity-related terms have smaller integration domains because the flow regions with the high vorticity are usually more compact. However, from a viewpoint of application, the local acceleration term in Eq. (3) is directly estimated because $\partial \mathbf{u} / \partial t$ can be more easily measured than $\partial \boldsymbol{\omega} / \partial t$ by using global velocimetry techniques in experiments. However, the shortcoming is that $\partial \mathbf{u} / \partial t$ decays much slower than $\partial \boldsymbol{\omega} / \partial t$ in the far field. It is necessary to estimate the asymptotic behavior of the acceleration term in Eq. (3) in the far-field flow and examine whether it decays fast enough for accurate calculation. When the far field is considered as an inviscid flow with $\mathbf{u} = \nabla \phi$, for a fixed rectangular control volume, the acceleration term at the far field decays in the fashion of $S_0 |z| \partial(\nabla \phi) / \partial t \sim S_0 |z|^{-n} \rightarrow 0$ as $|z| \rightarrow \infty$. The error term R_m will be further discussed in Sec. IV.D on a correction scheme.

The correctness of Eq. (3) is further examined from a theoretical standpoint. A rational approach is to check whether or not Eq. (3) is reduced to the well-known von Kármán–Sears lift formula for a thin airfoil in an unsteady inviscid flow [27]. For a two-dimensional (2-D) attached flow over a thin airfoil at suitably high Reynolds numbers, the flowfield is decomposed into a boundary layer and an outer potential flow. By applying Eq. (3) to this case, the lift per unit span is expressed as $L' \approx L'_{\text{vor}} + L'_a$, where L'_{vor} is the vortex lift, and L'_a is the added-mass lift. In the reduction of Eq. (3), the boundary layer is naturally reduced to a vortex sheet as a key element in unsteady thin airfoil theory, providing an insight into the physical foundation of thin airfoil theory. Further, to incorporate the wake effect into the theory, a decomposition of the vortex sheet strength $\gamma = \gamma_0 + \gamma_1$ is used, where γ_0 is the quasi-steady part without considering the effect of the wake, and γ_1 is the unsteady part induced by the wake. Therefore, a triple decomposition of the lift is obtained, where the first term is the quasi-steady vortex lift (the Kutta–Joukowski lift), the second term is the added-mass lift, and the third term is the wake-induced term. This result derived from Eq. (3) is a generalized version of the von Kármán–Sears lift formula with a general wake model. For the specific Green's function in the wake integral given by von Kármán and Sears [27], the lift formula derived from Eq. (3) for a thin airfoil can be mathematically reduced to the classical von Kármán–Sears lift formula.

Theoretically speaking, Eq. (3) is valid for a stationary or moving wing with the general geometry and kinematics in a steady freestream flow. Nevertheless, a question is how to clarify the generality of Eq. (3) for different geometrical parameters like camber and planform and kinematical parameters like waveform, flapping amplitude, phase, and frequency. This problem can be discussed based on the unsteady thin-airfoil theory as the first-order approximation of Eq. (3) for an attached flow. The sectional lift of a thin airfoil can be explicitly expressed by a general functional form that is a summation of the quasi-steady vortex lift, added-mass lift, and wake term. This triple decomposition of the lift originally given by von Kármán and Sears [27] is generically valid in the context of viscous flows. The effects of the wing camber and kinematics on the quasi-steady vortex lift and the added-mass lift can be directly estimated through the quasi-steady vortex sheet strength. Their effect on the wake term can be also estimated. Furthermore, the

effect of the wing planform could be evaluated by using a combination of the classical lifting-line theory and the unsteady thin-airfoil theory. Although the previous arguments are based on a reduced case of Eq. (3), they provide an insight into the generality of Eq. (3).

B. Momentum Form and Flux Form Force Formulas

Noca et al. [22] have derived three equivalent force expressions: momentum equation, flux equation, and impulse equation. The momentum equation is given by

$$\begin{aligned} F = & \underbrace{-\rho \frac{d}{dt} \int_{V_f} \mathbf{u} dV}_{A} + \underbrace{\rho \oint_{\Sigma} \frac{q^2}{2} \mathbf{n} dS}_{B} - \underbrace{\rho \oint_{\Sigma} \mathbf{n} \cdot (\mathbf{u} - \mathbf{u}_{\Sigma}) \mathbf{u} dS}_{C} \\ & - \underbrace{\frac{\rho}{k} \oint_{\Sigma} \mathbf{n} \cdot \mathbf{u} (\mathbf{x} \times \boldsymbol{\omega}) dS}_{D} + \underbrace{\frac{\rho}{k} \oint_{\Sigma} \mathbf{n} \cdot \boldsymbol{\omega} (\mathbf{x} \times \mathbf{u}) dS}_{E} - \underbrace{\frac{\rho}{k} \oint_{\Sigma} \left(\mathbf{x} \cdot \frac{\partial \mathbf{u}}{\partial t} \right) \mathbf{n} dS}_{F} \\ & + \underbrace{\frac{\rho}{k} \oint_{\Sigma} (\mathbf{n} \cdot \mathbf{x}) \frac{\partial \mathbf{u}}{\partial t} dS}_{G} + \underbrace{\frac{1}{k} \oint_{\Sigma} [\mathbf{x} \cdot (\nabla \cdot \boldsymbol{\tau})] \mathbf{n} dS}_{H} - \underbrace{\frac{1}{k} \oint_{\Sigma} (\mathbf{n} \cdot \mathbf{x}) (\nabla \cdot \boldsymbol{\tau}) dS}_{I} \\ & + \underbrace{\oint_{\Sigma} \mathbf{n} \cdot \boldsymbol{\tau} dS}_{J} - \underbrace{\rho \oint_{\partial B} \mathbf{n} \cdot (\mathbf{u} - \mathbf{u}_{\partial B}) \mathbf{u} dS}_{K} \end{aligned} \quad (4)$$

where \mathbf{u}_{Σ} and $\mathbf{u}_{\partial B}$ are the deforming velocities of the control surface, $k = N - 1$, and $N = 2, 3$ is the spatial dimensionality. The term A in Eq. (4) is the time rate of change of the momentum in the control volume. The terms $B - J$ represent the contributions from many flux terms on the outer control surface Σ . It will be pointed out that the terms C, D , and G are the dominant terms in addition to the term A . The term C is a flux of the relative momentum, the term D is the flux of the vorticity moment, and term G is the flux of the local acceleration. The term K is the relative momentum flux on the surface of a body.

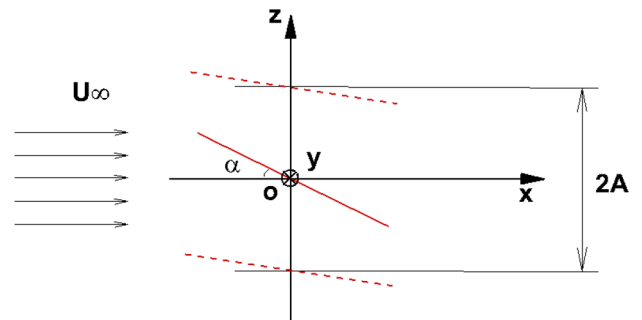


Fig. 1 Flapping flat plate and coordinate system.

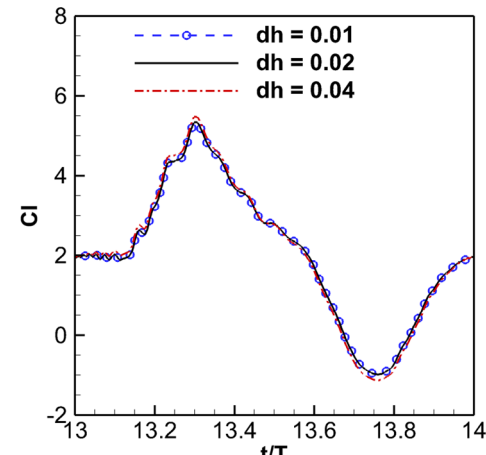


Fig. 2 Independence of the lift coefficient on the grid resolution for the flow over a flapping plate.

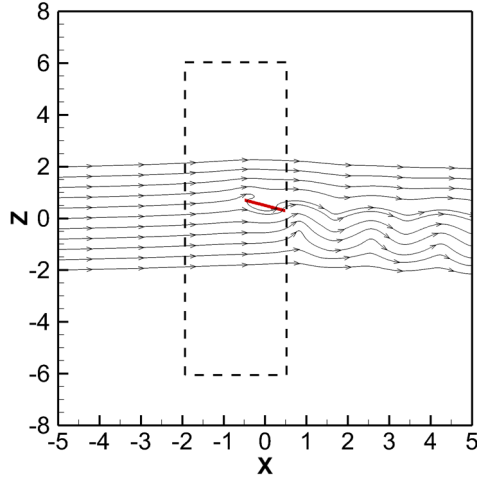


Fig. 3 Schematic of a rectangular control volume.

The flux equation is given by

$$\begin{aligned}
 F = & \underbrace{\rho \oint_{\Sigma} \frac{q^2}{2} \mathbf{n} dS}_{A} - \underbrace{\rho \oint_{\Sigma} \mathbf{n} \cdot \mathbf{u} \mathbf{u} dS}_{B} \\
 & - \underbrace{\frac{\rho}{k} \oint_{\Sigma} \mathbf{n} \cdot \mathbf{u} (\mathbf{x} \times \boldsymbol{\omega}) dS}_{C} + \underbrace{\frac{\rho}{k} \oint_{\Sigma} \mathbf{n} \cdot \boldsymbol{\omega} (\mathbf{x} \times \mathbf{u}) dS}_{D} \\
 & - \underbrace{\frac{\rho}{k} \oint_{\Sigma} \left(\mathbf{x} \cdot \frac{\partial \mathbf{u}}{\partial t} \right) \mathbf{n} dS}_{E} + \underbrace{\frac{\rho}{k} \oint_{\Sigma} (\mathbf{n} \cdot \mathbf{x}) \frac{\partial \mathbf{u}}{\partial t} dS}_{F} - \underbrace{\rho \oint_{\Sigma} \mathbf{n} \cdot \left(\frac{\partial \mathbf{u}}{\partial t} \mathbf{x} \right) dS}_{G} \\
 & + \underbrace{\frac{1}{k} \oint_{\Sigma} [\mathbf{x} \cdot (\nabla \cdot \boldsymbol{\tau})] \mathbf{n} dS}_{H} - \underbrace{\frac{1}{k} \oint_{\Sigma} (\mathbf{n} \cdot \mathbf{x}) (\nabla \cdot \boldsymbol{\tau}) dS}_{I} + \underbrace{\oint_{\Sigma} \mathbf{n} \cdot \boldsymbol{\tau} dS}_{J} \\
 & - \underbrace{\rho \oint_{\partial B} \mathbf{n} \cdot (\mathbf{u} - \mathbf{u}_{\partial B}) \mathbf{u} dS}_{K} - \underbrace{\rho \frac{d}{dt} \oint_{\partial B} \mathbf{n} \cdot (\mathbf{u} \mathbf{x}) dS}_{L} \quad (5)
 \end{aligned}$$

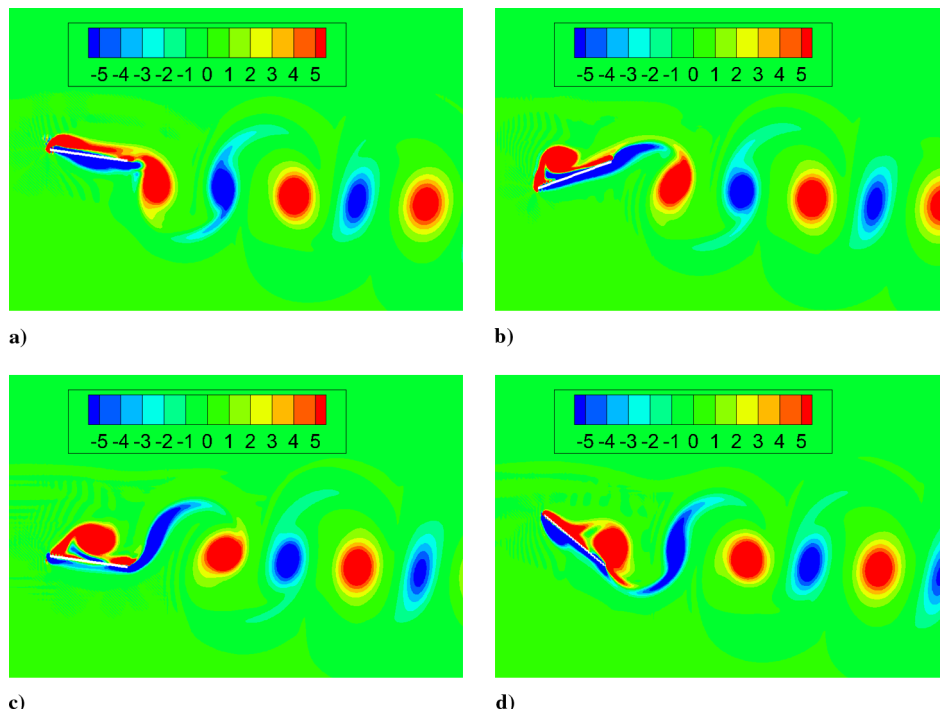


Fig. 4 Flow structures around the flapping plate at t/T equal to a) 12.25, b) 12.50, c) 12.75, and d) 13.0, where the grayscale (color online) indicates the normalized vorticity.

In Eq. (5), the force is mainly determined by the quantities on the surface of the control volume. Using the flux equation, Baik et al. [28] evaluated the terms in Eq. (5) to identify the contributions from vortical structures and acceleration. Actually, the terms A and B lead to the Lamb vector integral (see Appendix A). Based on some transformations, it can be found that the terms $C - G$ together can be mainly interpreted as the acceleration term. The terms $H - J$ represent the overall effect of the fluid viscosity on the outer control surface. The terms $K - L$ are related to the velocity and acceleration of the body surface. From Eqs. (4) and (5), the lift and drag are given by $F_z = \mathbf{k} \cdot \mathbf{F}$ and $F_x = \mathbf{i} \cdot \mathbf{F}$, respectively. The impulse equation of Noca et al. [22] can be transformed to Eqs. (4) and (5).

C. Advection Form Force Formula

Wu et al. [24] have derived several force formulas via the derivative-moment transformations. The advection form of the force formula is given by

$$\begin{aligned}
 \mathbf{F} = & \underbrace{-\frac{\rho}{k} \int_{V_f} \mathbf{x} \times \frac{\partial \boldsymbol{\omega}}{\partial t} dV}_{A} + \underbrace{\rho \int_{V_f} \mathbf{u} \times \boldsymbol{\omega} dV}_{B} + \underbrace{\frac{\rho}{k} \oint_{\partial V_f} \mathbf{x} \times \mathbf{n} \times (\mathbf{u} \times \boldsymbol{\omega}) dS}_{C} \\
 & - \underbrace{\frac{\mu}{k} \oint_{\Sigma} \mathbf{x} \times \mathbf{n} \times (\nabla \times \boldsymbol{\omega}) dS}_{D} + \underbrace{\mu \oint_{\Sigma} \boldsymbol{\omega} \times \mathbf{n} dS}_{E} + \underbrace{\frac{\rho}{k} \oint_{\partial B} \mathbf{x} \times \mathbf{n} \times \mathbf{a}_B dS}_{F} \quad (6)
 \end{aligned}$$

where $\partial V_f = \partial B + \Sigma$ denotes the control volume boundary (surface), \mathbf{x} is the positional vector, \mathbf{a}_B is the acceleration at the surface of a body, and $k = N - 1$, in which $N = 2$ or 3 is the number of the spatial dimensionality. The term A is related to the moment of the time derivative of the vorticity, and the term B is the vortex force. The term C is related to the moment of the Lamb vector relative to the positional vector $\mathbf{x} \times \mathbf{n}$ on the control surface. The terms D and E are the contributions of flow structures on the outer control surface through a pure viscous effect. The term F is related to the moment of the acceleration \mathbf{a}_B relative to the positional vector $\mathbf{x} \times \mathbf{n}$ on the surface of a body.

In the derivation of Eq. (6) in Appendix A, the acceleration term in Eq. (2) is converted to the vorticity-related terms, and the total pressure term in Eq. (2) is exactly canceled out. Therefore, Eq. (6) enjoys the

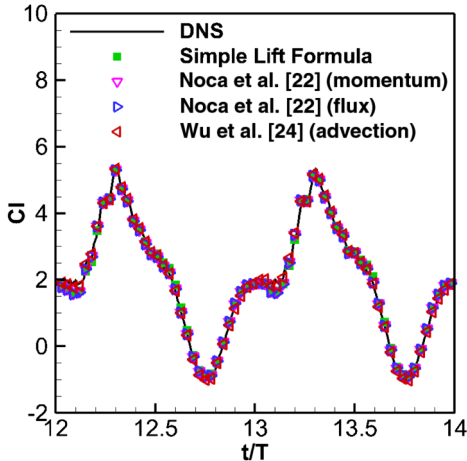


Fig. 5 Time histories of the lift coefficient of the flapping plate obtained by using the different lift formulas.

generality and some advantages from a theoretical viewpoint. The distinct advantage is that the lift calculation is insensitive to the size and shape of the control volume because the vorticity domain is more compact. The terms A and C together in Eq. (6) are the main contributions to the acceleration term and the total pressure term [the terms A , C , and D in Eq. (2)]. Therefore, the contribution of the terms A and C together in Eq. (6) to the lift approximately equals that of the acceleration term in Eq. (2), and their contribution to the drag is approximately equivalent to the parasite drag plus the acceleration term projected onto the freestream direction.

III. Kinematical Model and Numerical Method

A. Flapping Plate and Rectangular Wing

The 2-D flow and lift of a flapping plate with infinite wingspan is first investigated. The plate has a chord length c and zero thickness, heaving vertically and rotating around the center of the plate in a uniform flow. The Cartesian system ($o-xyz$) fixed in the space is used. As shown in Fig. 1, the x axis directs downstream in parallel to the freestream, the z axis is perpendicular to the freestream pointing upward, and the y axis is normal to the $x-z$ plane along the wingspan. The kinematics of the flapping plate is described by the pitching angle (angle of attack, or AoA) and the vertical position of the center of the plate, i.e.,

$$\alpha = \alpha_0 + \alpha_m \cos(2\pi ft) \quad (7)$$

$$z_c = z_{c0} + A \sin(2\pi ft) \quad (8)$$

In Eq. (7), α is the instantaneous AoA, $\alpha_0 = 10$ deg is the time-averaged AoA, and $\alpha_m = 30$ deg is the pitching amplitude. In Eq. (8), z_c is the vertical position of the center of the plate, $z_{c0} = 0$ is the time-averaged vertical position of the center, and $A = 0.25c$ is the heaving amplitude. $f = 0.6(U_\infty/c)$ is the pitching and/or heaving frequency. The Strouhal number of the flapping wing is defined as $St = (2fA)/U_\infty = 0.3$. For the flapping rectangular wing with the finite aspect ratio of $AR = 4.0$, the geometrical and kinematical settings remain the same as these for the flapping plate.

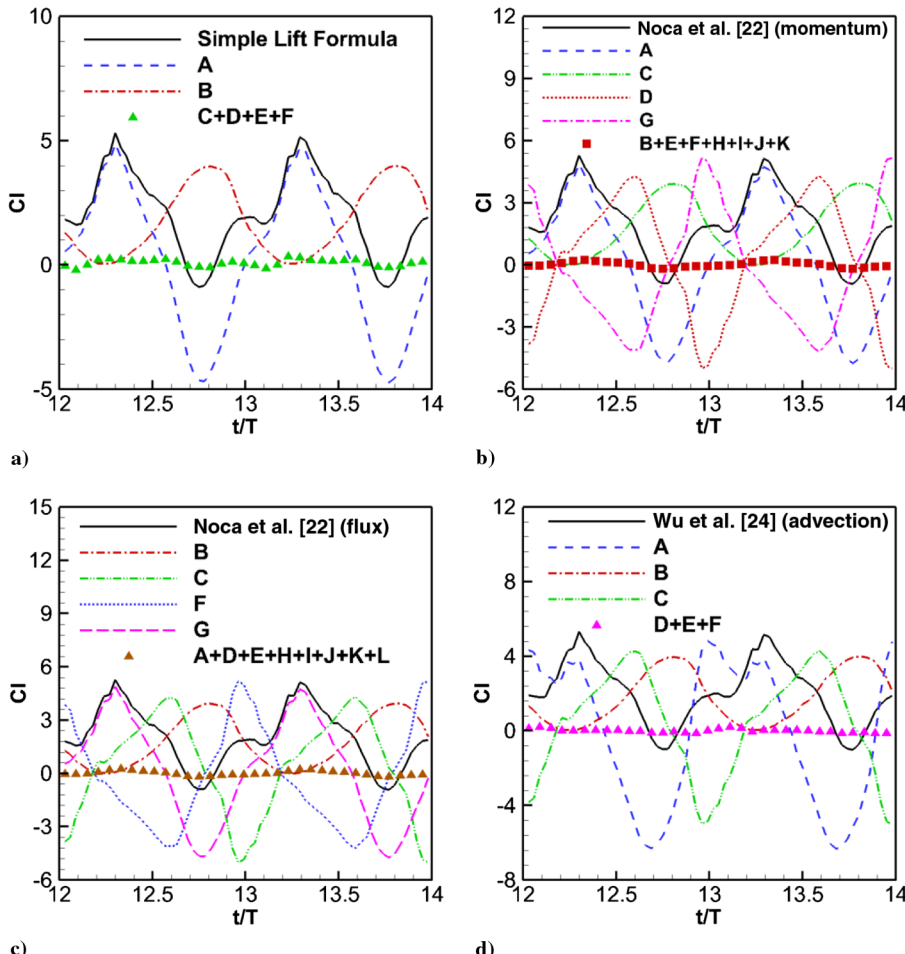


Fig. 6 Contributions of the terms to the lift coefficient of the flapping plate in the different lift formulas.

Table 1 Error of lift coefficient of the flapping plate

Formula	Dominant terms	$\ \Delta Cl\ _2$	$\ Cl\ _2$	$\ \Delta Cl\ _2/\ Cl\ _2, \%$
Simple lift formula	A, B	0.13	2.69	5
Noca et al. [22] (momentum)	A, C, D, G	0.13	2.69	5
Noca et al. [22] (flux)	B, C, F, G	0.13	2.69	5
Wu et al. [24] (advection)	A, B, C	0.09	2.69	3

B. Numerical Method

The flow around the flapping plate/rectangular wing is determined by the incompressible Navier–Stokes equations:

$$\frac{\partial \mathbf{u}}{\partial t} + \mathbf{u} \cdot \nabla \mathbf{u} = -\nabla p + \frac{1}{Re} \nabla^2 \mathbf{u} + \mathbf{f} \quad (9)$$

$$\nabla \cdot \mathbf{u} = 0 \quad (10)$$

where \mathbf{u} is the velocity, p is the pressure, and \mathbf{f} is the body force representing the effects of the boundaries on the flow. All the variables are nondimensional based on U_∞ and c . The Reynolds number based on the chord length of the plate and uniform upstream flow is $Re = U_\infty c / \nu = 300$. The unsteady flows with the moving boundaries are simulated by using the immersed boundary method based on the discrete stream function formulation developed by Wang and Zhang [29]. In this method, the discrete stream function method (or exact projection method, null space method) proposed by Chang et al. [30] is used to solve the Navier–Stokes equations on a Cartesian Eulerian grid. The geometry and kinematics of the moving boundaries are described by a Lagrangian grid. The effects of the boundaries on the flow are represented by adding a force term \mathbf{f} in Eq. (9). The force term \mathbf{f} is determined by solving a linear system regarding the interpolation between the Lagrangian and Eulerian grid points, i.e.,

$$\begin{aligned} & \sum_{j=1}^M \left(\sum_x \delta_h(\mathbf{x} - \mathbf{X}_j) \delta_h(\mathbf{x} - \mathbf{X}_k) (\delta s)^2 (\delta h)^3 \right) \mathbf{F}(\mathbf{X}_j) \\ &= \frac{\mathbf{U}^{n+1}(\mathbf{X}_k) - \mathbf{U}^*(\mathbf{X}_k)}{\Delta t} \end{aligned} \quad (11)$$

$$\mathbf{f}(\mathbf{x}) = \sum_{j=1}^M \mathbf{F}(\mathbf{X}_j) \delta_h(\mathbf{x} - \mathbf{X}_j) (\delta s)^2 \quad (12)$$

where \mathbf{x} and \mathbf{X} are the position vectors of the Eulerian and Lagrangian grid points, respectively; \mathbf{F} is the force at the Lagrangian grid points; $\mathbf{U}^{n+1}(\mathbf{X}_k)$ and $\mathbf{U}^*(\mathbf{X}_k)$ are the desired velocity and predicted velocity at the k th Lagrangian grid point, respectively; δ_h is the discrete delta function the form provided by Peskin [31] is used in the present simulations; δh and δs are the Eulerian and Lagrangian grid size, respectively; and M is the number of the Lagrangian grid points. The validations and the details of the numerical method can be found in our previous work for various flows [26,29].

The computational domain used in the present work is $[-12, 20] \times [-16, 16]$ in the streamwise (x) direction and vertical (z) direction for 2-D flows, and $[-12, 20] \times [-16, 16] \times [-16, 16]$ in the streamwise (x), spanwise (y), and vertical (z) directions for three-dimensional (3-D) flows. The unstructured Cartesian mesh with the hanging nodes is used in the simulations to refine the mesh around the plate. The minimum grid size is $dh = 0.02$, and the maximum grid size is $dh = 0.32$. The time step is selected to keep the maximum Courant–Friedrichs–Lowy number at 0.5. The independence of the lift coefficient on the grid resolution for the flow over the flapping plate is shown in Fig. 2. In all the simulations, the uniform upstream flow is set at the inlet, and the free convection flow at the outlet. The nonslip boundary condition is specified at the surface of the plate/rectangular

wing. The symmetric boundary conditions are used at other boundaries. The initial condition for the flow is $(U_\infty, 0, 0)$. A rectangular control volume is used in the present work. As shown in Fig. 3, the top and bottom boundaries of the control volume are at $z = \pm 6$. The left boundary is at $x = -2$, and the right boundary is at $x = x_t$, where x_t is the maximum streamwise position of the trailing edge. In the rectangular-wing case, the side boundaries of the control volume are at $y = \pm 6$.

IV. Results and Discussions

A. Flapping Plate

The flows over the flapping plate are unsteady. The vortices shed from the plate and rectangular wing. Figure 4 shows the normalized spanwise vorticity fields [$\omega^* = \omega(c/U_\infty)$] around the flapping plate in one period, which illustrates the evolution of the flow structures at four instants. At $t/T = 12.25$ and 12.50 , the center of the plate is at

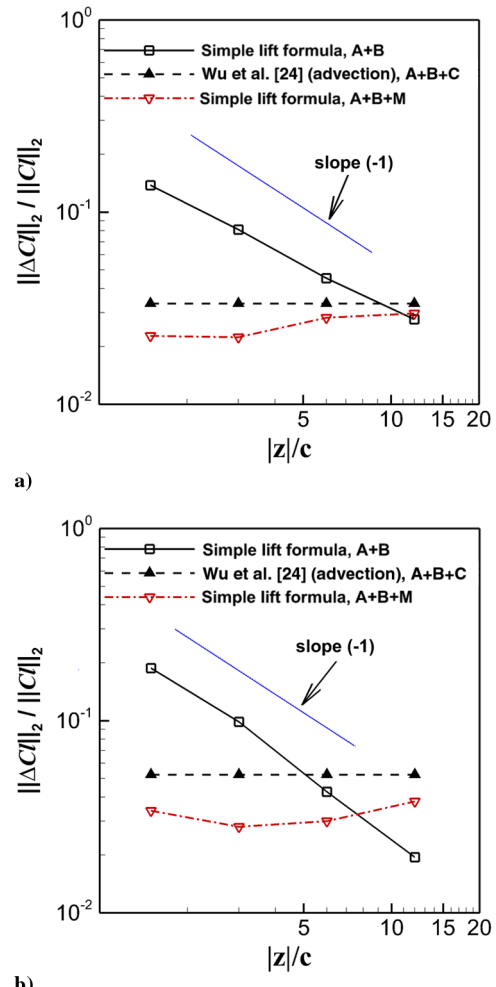


Fig. 7 Relative error of a) the flapping flat plate, and b) the flapping rectangular wing, where M in the label denotes the correction model term.

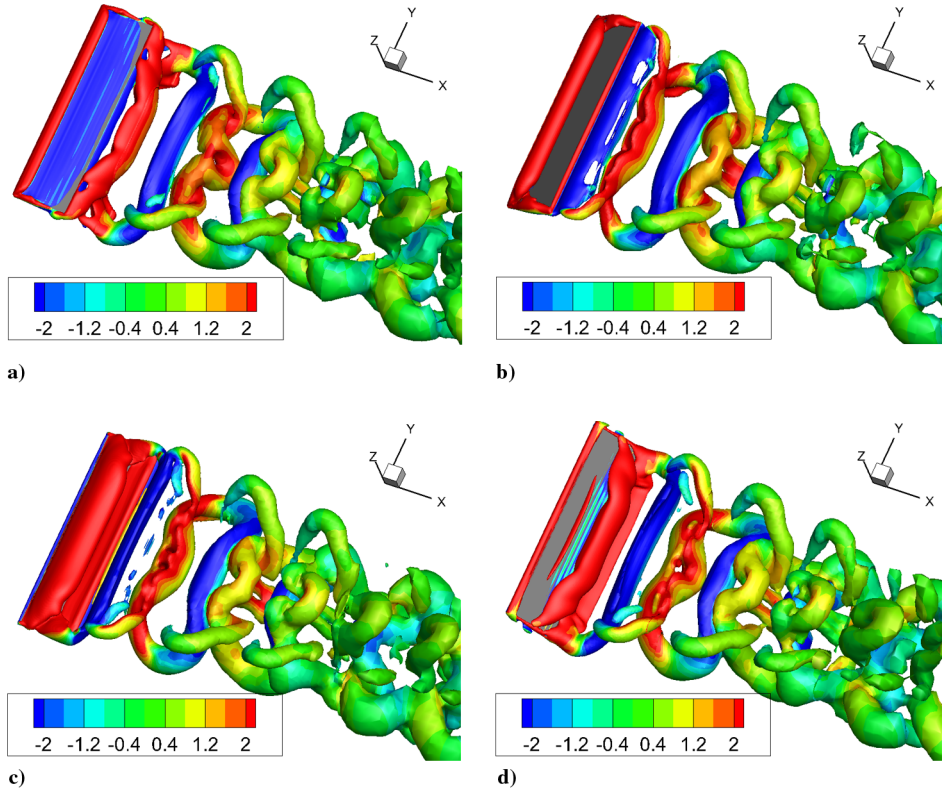


Fig. 8 Flow structures ($Q = 1$) at t/T equal to a) 6.25, b) 6.50, c) 6.75, and d) 7.0, where the grayscale (color online) indicates the normalized vorticity.

the maximum position in vertical direction and at the middle position and moving toward downward. At $t/T = 12.75$ and 13.0, the center of the plate is at the minimum position in the vertical direction and at the middle position and moving toward upward. In the downstroke, the flow on the upper surface of the plate separates at the leading edge. The shear layer from the leading edge rolls up and forms the leading-edge vortex (LEV) with positive vorticity on the upper surface of the plate. This LEV stays on the upper surface of the plate for about a half of a period and merges with the trailing-edge vortex in the upstroke. In the upstroke, an LEV with negative vorticity forms and stays for about a half of a period on the lower surface of the plate. It merges with the trailing-edge vortex generated in the next downstroke. The LEV generated in the upstroke is weaker than that generated in the downstroke because of a smaller relative angle of attack in the upstroke. The LEV corresponds to a region of low pressure. The LEV on the upper surface of the plate leads to an increase in lift, whereas the LEV on the lower surface causes a decrease in lift.

The previous observation is consistent with the variation of the lift coefficient shown in Fig. 5, indicating that the lift coefficient in the downstroke is much larger than that in the upstroke. The lift coefficient used in this work is defined as $C_l = F_z / 0.5 \rho U_\infty^2 S$, where S is the area of the wing ($S = 1 \cdot c$ for the plate and $S = ARc^2$ for the rectangular wing). Figure 5 shows the lift coefficients calculated by using the five different lift formulas. The lift coefficient given by using Eq. (1) is labeled as “DNS”. The lift coefficients calculated by using Eqs. (2) and (4–6) are labeled as “simple lift formula”, “Noca et al. [22] (momentum)”, “Noca et al. [22] (flux)”, and “Wu et al. [24] (advection)”, respectively. It is shown that all the lift formulas give the lift coefficients that are in good agreement with DNS. This indicates that Eqs. (2) and (4–6) can predict the lift coefficient when a velocity field with a sufficiently high resolution is provided. However, a practical question is how many dominant terms in a lift formula are required to calculate the lift with a sufficient accuracy. From a standpoint of application, a good lift formula should have a minimal number of dominant terms with lucid physical meanings.

The force formulas [Eqs. (2) and (4–6)] have different forms, although they are equivalent mathematically as indicated in

Appendix A. The dominant terms in these lift formulas are identified based on DNS data for the flapping plate. Figure 6 shows the contributions of all the terms in Eqs. (2) and (4–6) to the lift coefficient in one period. For a rectangular control volume, as shown in Fig. 6a, Eq. (2) has only two dominant terms (A and B), and the sum of the remaining terms (C , D , E , and F) is much smaller. Thus, Eq. (2) is reduced to the simple lift formula [Eq. (3)]. The term A is the vortex lift, and the term B is the contribution of the local acceleration associated with the induced unsteady velocity by the motion of the plate. The relative errors $\|\Delta C_l\|_2 / \|C_l\|_2$ of the lift coefficients given by the dominant terms in these lift formulas are summarized in Table 1, where $\|C_l\|_2$ is the L2-norm of C_l , and $\|\Delta C_l\|_2$ is the L2-norm of the error of ΔC_l . The error in the lift prediction by using the simple lift formula with the two dominant terms is 5%. Here, the L2-norm is defined as

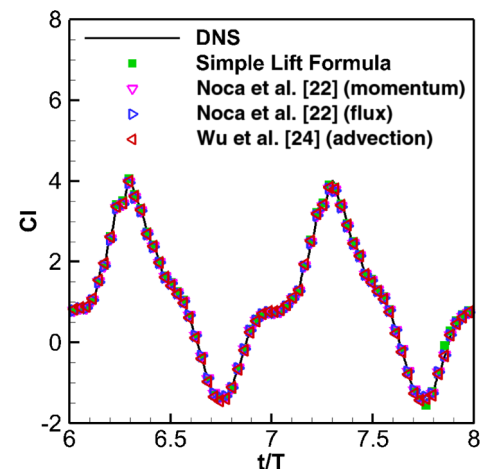


Fig. 9 Time histories of the lift coefficient of a flapping rectangular wing obtained by using the different lift formulas.

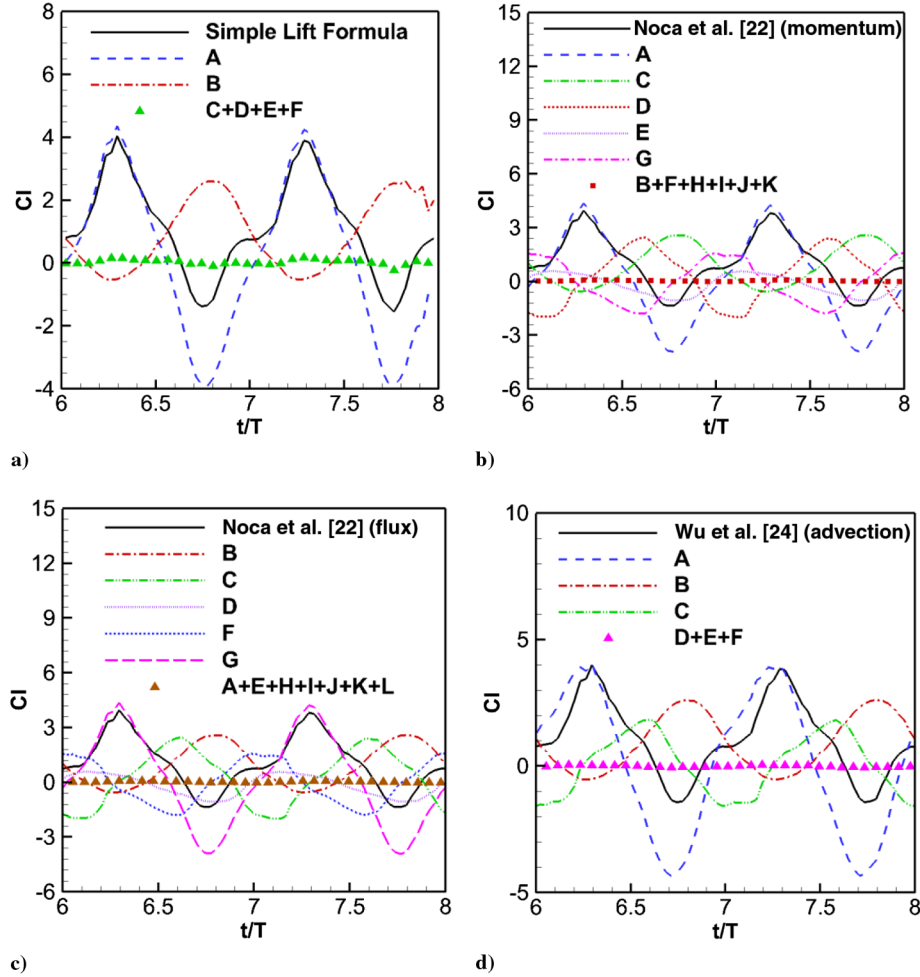


Fig. 10 Contributions of the terms to the lift coefficient of the flapping rectangular wing in the different lift formulas.

$$\|\bullet\|_2 = \left(\sum_{i=1}^N (\bullet)_i^2 / N \right)^{1/2}$$

where $N = 32$ in one period.

The momentum equation [Eq. (4)] given by Noca et al. [22] has four dominant terms (A , C , D , and G) when it is used in calculating the lift of the flapping plate, as shown in Fig. 6b. The contributions from these dominant terms are in the same order. The term A indicates the contribution to the lift by the time rate of change of the momentum in the control volume. The terms C , D , and G nominally represent the contributions from the fluxes of the relative momentum, vorticity moment, and local acceleration across the outer control surface, respectively. The term E is zero in 2-D flows because the vorticity is perpendicular to the normal direction of the control surface. The term K is zero because the nonslip boundary condition is used on the surface of the plate. The contributions of all the remaining terms are small, and the sum of these terms is plotted in Fig. 6b. Similarly, as shown in Fig. 6c, the flux equation [Eq. (5)] given by Noca et al. [22] has four dominant terms (B , C , F , and G) in this case. Nominally,

dominant terms B , C , and $F + G$ can be interpreted as the fluxes of the momentum, vorticity moment, and local acceleration across the outer control surface, respectively. The term D is related to the flux of vorticity on the outer control surface, and it is zero for 2-D flows. The term K is zero because of the nonslip boundary condition on the surface of the plate. The term L is zero because a rigid plate with the zero thickness is used in this work. All the remaining terms contribute little contribution to the lift. The main difficulty of application of the momentum and flux equations given by Noca et al. [22] is that the connection between these terms (particularly the flux terms on Σ) and the flow structures near the plate is not clear, such that the contributions from the identified flow structures near the airfoil/wing to lift generation cannot be easily estimated and interpreted.

The advection form of the force formula [Eq. (6)] given by Wu et al. [24] has three dominant terms (A , B , and C), as shown in Fig. 6d. The term A is the contribution of the moment of the time derivative of the vorticity, and the term B is the vortex force. The term C is related to the flux of the moment of the Lamb vector on the control surface. The term F is zero because of the rigid plate with zero thickness used in this work. The terms D and E contribute little to the lift, as shown in

Table 2 Error of lift coefficient of the flapping rectangular wing

Formula	Dominant terms	$\ \Delta Cl\ _2$	$\ Cl\ _2$	$\ \Delta Cl\ _2 / \ Cl\ _2, \%$
Simple lift formula	A, B	0.08	1.91	4
Noca et al. [22] (momentum)	A, C, D, E, G	0.04	1.91	2
Noca et al. [22] (flux)	B, C, D, F, G	0.04	1.91	2
Wu et al. [24] (advection)	A, B, C	0.10	1.91	5

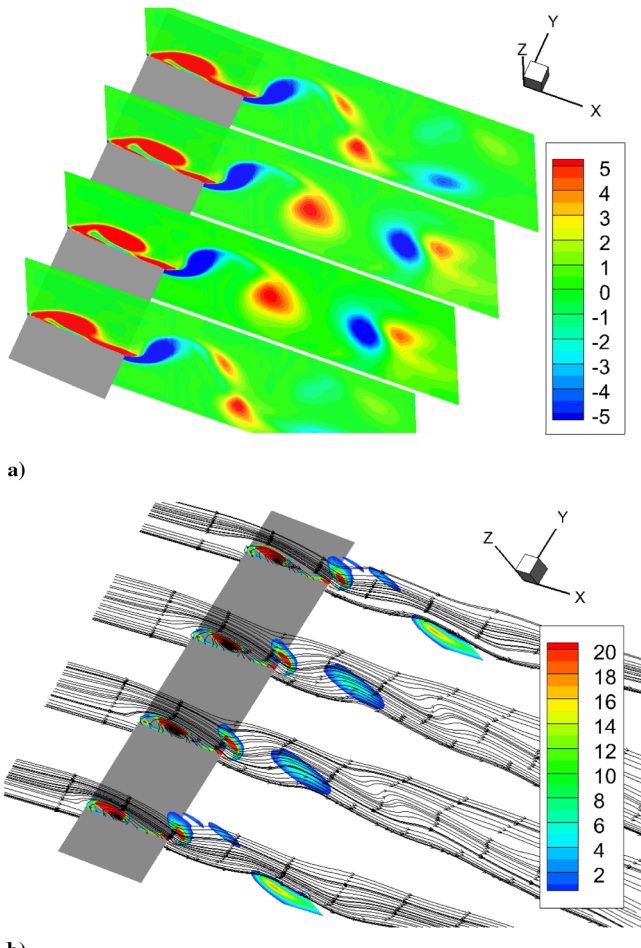


Fig. 11 Typical planar fields at different spanwise locations:
a) normalized vorticity, and b) normalized second invariant and streamlines.

Fig. 6d. In this case, the total contribution from the terms A and C is basically equivalent to the local acceleration term in Eq. (3). As shown in Table 1, the relative errors of the lift coefficient defined as $\|\Delta Cl\|_2/\|Cl\|_2$ given by the dominant terms in the lift formulas of Noca et al. (momentum and flux) and Wu et al. (advection) are 5% and 3%, respectively. In Appendix B, the dominant terms contributing to the drag coefficient in the different force formulas are also identified.

It is indicated in Sec. II.B that the accuracy of the simple lift formula depends on the distance between the upper or lower face of the rectangular control volume and the wing. For a larger distance, the error associated with the neglected total pressure term and the error in calculation of the acceleration term are smaller. It is necessary to quantify the error as a function of the distance. Figure 7 shows the relative error $\|\Delta Cl\|_2/\|Cl\|_2$ as a function of the normalized distance between the upper or lower face of the rectangular control volume and the wing for the flapping flat plate and the flapping rectangular flat-plate wing. The error of the simple lift formula exhibits a power-law decay, i.e., $\|\Delta Cl\|_2/\|Cl\|_2 \propto (|z|/c)^{-n}$, where n is about 1 for both the cases, and $|z|$ denotes the distance between the upper or lower face of the control surface and the wing. For the flapping flat plate, $\|\Delta Cl\|_2/\|Cl\|_2$ decreases from about 4.5% for $|z|/c = 6$ to 2.5% for $|z|/c = 12$. The dependency of the error in lift calculation on the size of the domain is considered as a shortcoming of the simple lift formula, which is not known a priori depending on the flow. In contrast, the error in lift calculation given by the dominant terms in the advection form of the force formula of Wu et al. [24] does not depend on the distance, and it is about 3.5%. For the flapping rectangular wing, the error of the simple lift formula is about 4% for $|z|/c = 6$, which is comparable to 5% for the advection form of the force formula of Wu et al.

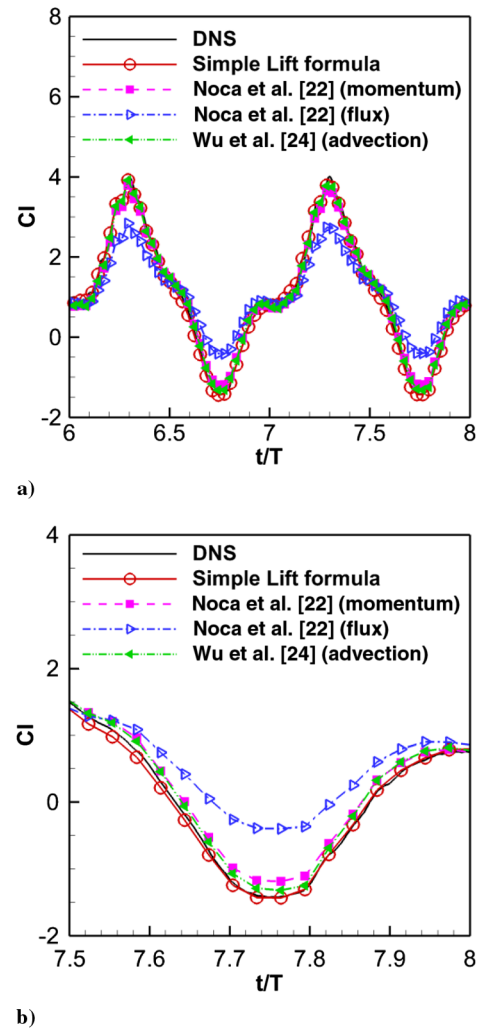


Fig. 12 Time histories of the lift coefficients of a flapping rectangular wing in a) two periods, and b) zoomed-in time span.

B. Flapping Rectangular Wing

The lift formulas are further evaluated based on the 3-D unsteady flow over the flapping rectangular wing. Figure 8 shows the 3-D flow structures visualized by the isosurface of $Q = 1.0$ around the flapping rectangular wing in one period at $t/T = 6.25, 6.50, 6.75$, and 7.0, where Q is the second invariant of the velocity gradient sensor, and the grayscale (color online) indicates the normalized vorticity. At $t/T = 6.25$ and 6.5, the center of the plate is at the maximum position in the vertical direction and at the middle position, which is moving downward. At $t/T = 6.75$ and 7.0, the center of the plate is at the minimum position in the vertical direction and at the middle position, which is moving upward. The evolution of the 3-D flow structures around the flapping rectangular wing is similar to those around the flapping plate, except that a pair of the tip vortices is generated in the downstroke and upstroke due to the finite wingspan. As shown in Fig. 8, the LEV, tip vortices, and trailing-edge vortices generated in each flapping cycle (the downstroke and upstroke) form a vortex ring, resulting in a chain of the braided vortex rings in the near-wake. As shown in Fig. 9, the smaller relative angle of attack in the upstroke causes a weaker vortex ring, which corresponds to the smaller magnitude of the negative lift coefficient. In the downstroke, a stronger vortex ring is induced at the larger relative angle of attack, which corresponds to the larger magnitude of the positive lift coefficient.

Figure 9 shows the time histories of the lift coefficient of the flapping rectangular wing obtained by using the different lift formulas. Like the 2-D case, all the lift formulas give predictions of the lift that are in good agreement with DNS. Figure 10 shows the contributions of the terms to the lift coefficient of the flapping

Table 3 Error of lift coefficient with quasi-2-D approximation

Formula	Dominant terms	$\ \Delta Cl\ _2$	$\ Cl\ _2$	$\ \Delta Cl\ _2/\ Cl\ _2, \%$
Simple lift formula	A, B	0.21	1.91	11
Noca et al. [22] (momentum)	A, C, D, E, G	0.30	1.91	16
Noca et al. [24] (flux)	B, C, D, F, G	0.63	1.91	33
Wu et al. [24] (advection)	A, B, C	0.28	1.91	15

rectangular wing in the different lift formulas. As shown in Fig. 10a, the simple lift formula [Eq. (3)] has two dominant terms: the vortex lift and the local acceleration term. The momentum equation of Noca et al. [22], Eq. (4), has five dominant terms for 3-D flows. The term E in Eq. (4) that is related to the vorticity flux at the outer control surface cannot be neglected in this case because the vorticity is not necessary to be perpendicular to the normal vector of the control surface in 3-D flows. The flux equation of Noca et al. [Eq. (5)] also has five dominant terms for 3-D flows. Similarly, the contribution of the term D in Eq. (5) cannot be neglected in 3-D flows. As shown in Fig. 10d, the advection form of the force formula of Wu et al. [24] has three dominant terms in 3-D flows. Table 2 lists the relative errors $\|\Delta Cl\|_2/\|Cl\|_2$ of the lift coefficients given by the dominant terms in the lift formulas for the flapping rectangular wing. The simple lift formulas with only two dominant terms has an error of 4% compared to 2% for the five terms in the formulas of Noca et al. [22] and 5% for the three terms in the formula of Wu et al. [24]. Recently, the simple lift formula is applied to the complex flowfields around a flapping rectangular flat-plate wing with a dynamically changing wingspan, and it gives the histories of the unsteady lift that are consistent with DNS [32].

C. Simulated Particle-Image-Velocimetry Measurements

The lift formulas are useful because the lift could be estimated from velocity data obtained from PIV measurements. Standard planar PIV measurements are usually made at selected spanwise locations along a wing. The sectional lifts are obtained by using the lift formulas at these spanwise locations, and then the total lift of the wing is estimated by summing the sectional lifts. This approach is a quasi-2-D approximation of lift estimation by using the lift formulas. To evaluate the effect of the limited number of the spanwise locations in measured velocity fields on calculation of the lift by using the quasi-2-D approximation, PIV measurements on the flapping rectangular wing are simulated based on the DNS data. Figure 11 shows the normalized vorticity and second invariant fields on the cross sections (slices) at four spanwise locations on the flapping rectangular wing with $AR = 4$ for $Re_c = 300$ and $a_0 = 10$ deg, which simulate typical planar PIV measurements. Figure 12a shows the histories of the lift coefficient calculated by using the lift formulas with the dominant terms under the quasi-2-D approximation based on 31 slices of the velocity fields uniformly distributed in a spanwise region $[-3, 3]$. A zoomed-in view is given in Fig. 12b to show the differences between the lift formulas and the DNS results. The simple lift formula gives the best result, whereas the lift formula of Wu et al. [24] and the momentum equation of Noca et al. [22] give the fairly good results. The flux equation of Noca et al. has a larger error because the term D in Eq. (5) is zero in the quasi-2-D approximation, but in the real 3-D case, it is significant, as indicated in Fig. 10c. Table 3 gives a summary of the errors of the lift coefficient predicted by using the dominant terms in the different formulas under the quasi-2-D approximation for the flapping rectangular wing.

D. Correction for Small Control Domain

As pointed out before, the accuracy of the simple lift formula depends on the distance between the upper or lower face of the rectangular control surface and the wing. For a small distance (such as $|z|/c < 3$), the error could be significant. For example, $\|\Delta Cl\|_2/\|Cl\|_2$ is about 10% for $|z|/c = 1.2$. To compensate the far-field effects neglected by the simple lift formula for a small domain, a correction scheme is proposed to compensate the far-field effects neglected by the simple lift formula for a small domain. The error term R_m in the simple lift formula is evaluated, which is mainly

contributed by the far-field part neglected in the calculation of the acceleration term when the vertical distance of a control volume is small. An estimate of R_m is given by following nondimensional relation:

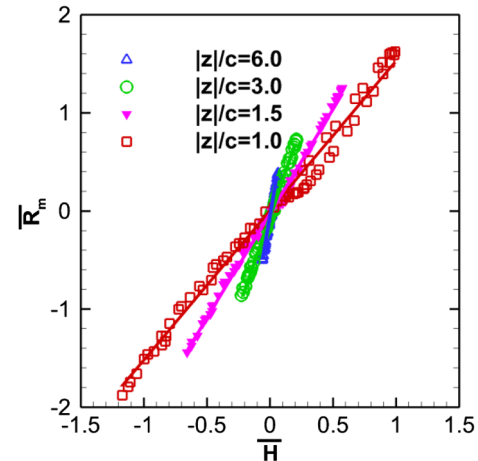
$$\bar{R}_m(|z|/c, t) = \frac{R_m(t)}{q_\infty S} = \beta(|z|/c) \bar{H}(|z|/c, t) \quad (13)$$

where $\bar{H} = cH/q_\infty S$ is a nondimensional function of

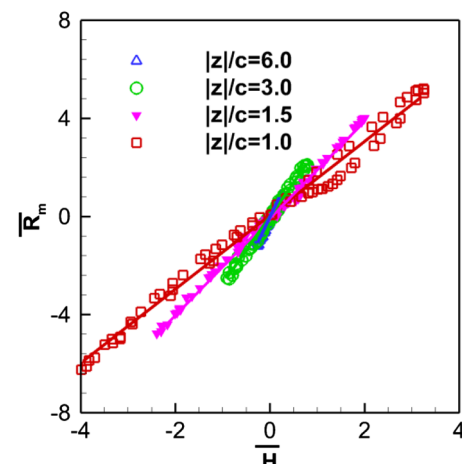
$$H = \rho S_0 \frac{\partial}{\partial t} (\langle u_z^+ \rangle_A + \langle u_z^- \rangle_A) \quad (14)$$

$|z|$ is the distance between the top or bottom face of a rectangular control surface and the wing, S_0 is the area of the top or bottom face, β is a factor, “+” and “−” denote the top and bottom faces, respectively, and

$$\langle \bullet \rangle_A = S_0^{-1} \int_{S_0} \bullet dS$$



a)



b)

Fig. 13 Relation between \bar{R}_m and \bar{H} at different domain sizes for a) the flapping plate, and b) the flapping rectangular wing.

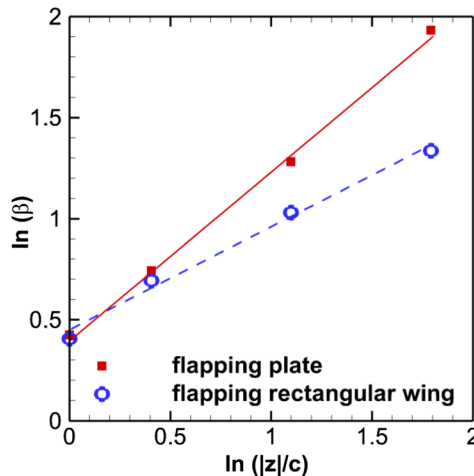


Fig. 14 Relation between β and $|z|/c$, where the solid and dashed lines show the linear regressions by $\ln(\beta) = 0.41 + 0.84 \ln(|z|/c)$ and $\ln(\beta) = 0.45 + 0.51 \ln(|z|/c)$, respectively.

is the area-averaging operator. Physically speaking, Eq. (13) represents the time rate of the integral far-field fluid momentum neglected in the simple lift formula for a small domain. As shown in Fig. 13, the linear relationship between $\bar{R}_m(|z|/c, t)$ and $\bar{H}(|z|/c, t)$ is validated numerically for the flapping flat plate and the flapping rectangular wing. The factor β is determined for different values of $|z|/c$. As shown in Fig. 14, there is a power-law relation $\beta = a(|z|/c)^n$, where n is an exponent, and a is a nondimensional coefficient. For the flapping plate, $n = 0.84$ and $a = 1.51$. For the flapping rectangular wing, $n = 0.51$ and $a = 1.57$. The universality of n and a should be further examined in the parametric space. Equations (13) and (14) provide a simple correction scheme based on the known velocity data on the top and bottom faces of a control surface to improve the accuracy of the simple lift formula for a small domain. Figure 7 shows the relative error of the corrected results by using Eqs. (13) and (14) in comparison with those without the correction ($R_m = 0$). The error of the corrected results is not only much smaller for a small domain but also almost independent of the size of the rectangular control surface.

V. Conclusions

The dominant terms in the four lift formulas are identified based on the DNS of the 2-D and 3-D unsteady flows over a flapping plate and a flapping rectangular wing at low Reynolds number. It is demonstrated that the simple lift formula with the vortex force and local acceleration terms can give a good prediction of the lift coefficient based on velocity fields obtained from computations and simulated planar PIV measurements. The physical meanings of these terms are clear in terms of the relevance of flow structures to lift generation. In the simulated PIV measurements where only planar velocity fields at several spanwise locations are available, the simple lift formula gives the reasonable result. The foundations of the lift formulas are equivalent mathematically, and these formulas just provide the lift decompositions from the different perspectives. However, from a standpoint of application, the simple lift formula provides a simple but sufficiently accurate way to estimate the lift from a velocity field and analyze the relationship between lift generation and flow structures.

Appendix A: Connections Between the Present and Other Force Expressions

A1 Equivalence Between Two Basic Force Expressions

Here, we want to show the equivalence between two basic fluid-mechanic force expressions: Eq. (1) in the present work and the expression given by Noca et al. [22] (Sec. 1.1 in their paper). Some

alternative, more convenient force expressions can be derived from the two basic expressions by using various transformations. This appendix discusses the intrinsic connections between the present force expression and those given by Noca et al. [22], Wu et al. [24], and Chang [20]. Consider the force acting on a body B moving arbitrarily in a fluid as shown in Fig. A1. The body surface is denoted by ∂B deforming with the velocity $\mathbf{u}_{\partial B}(t)$. The control volume $V_f(t)$ encloses the fluid between the body surface ∂B and the outer control surface Σ around the body that is moving with the velocity $\mathbf{u}_{\Sigma}(t)$. The unit normal vector \mathbf{n} points to the outside of the control surface. In an incompressible flow with constant density ρ , the rate of change of the momentum of the fluid in the control volume $V_f(t)$ is

$$\rho \frac{d}{dt} \int_{V_f(t)} \mathbf{u} dV \quad (A1)$$

The momentum flux through the control surface is

$$\rho \oint_{\partial B} \mathbf{u} (\mathbf{u} - \mathbf{u}_{\partial B}(t)) \cdot \mathbf{n} dS + \rho \oint_{\Sigma} \mathbf{u} (\mathbf{u} - \mathbf{u}_{\Sigma}(t)) \cdot \mathbf{n} dS \quad (A2)$$

and the force acting on the control surface is

$$\oint_{\partial B} (-pI + \tau) \cdot \mathbf{n} dS + \oint_{\Sigma} (-pI + \tau) \cdot \mathbf{n} dS \quad (A3)$$

The momentum balances for the control volume $V_f(t)$ gives the force acting on the body

$$\begin{aligned} \mathbf{F} &= - \oint_{\partial B} (-pI + \tau) \cdot \mathbf{n} dS \\ &= -\rho \frac{d}{dt} \int_{V_f(t)} \mathbf{u} dV - \rho \oint_{\partial B} \mathbf{u} (\mathbf{u} - \mathbf{u}_{\partial B}(t)) \cdot \mathbf{n} dS \\ &\quad - \rho \oint_{\Sigma} \mathbf{u} (\mathbf{u} - \mathbf{u}_{\Sigma}(t)) \cdot \mathbf{n} dS + \oint_{\Sigma} (-pI + \tau) \cdot \mathbf{n} dS \end{aligned} \quad (A4)$$

Equation (A4) is just the starting expression used by Noca et al. [22] in their derivations.

On the other hand, for an incompressible flow, direct application of Leibniz's rule for a 3-D case to a time-dependent control volume $V_f(t)$ leads to the following identity:

$$\frac{d}{dt} \int_{V_f(t)} \mathbf{u} dV = \int_{V_f(t)} \frac{D\mathbf{u}}{Dt} dV - \oint_{\partial V_f(t)} \mathbf{u} (\mathbf{u} - \mathbf{u}_{\partial V_f(t)}) \cdot \mathbf{n} dS \quad (A5)$$

where $\partial V_f = \partial B + \Sigma$ denotes the control volume boundary that moves with the velocity $\mathbf{u}_{\partial V_f(t)}$ [24]. The Reynolds transport theorem is a reduced form of Eq. (A5) when the control surface moves with the same velocity of the fluid as a material surface. Combination of Eqs. (A4) and (A5) yields

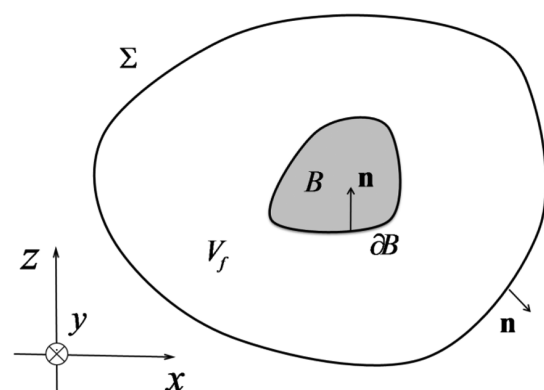


Fig. A1 Schematic of a control surface around a body.

$$\mathbf{F} = -\rho \int_{V_f(t)} \frac{D\mathbf{u}}{Dt} dV + \oint_{\Sigma} (-p\mathbf{I} + \boldsymbol{\tau}) \cdot \mathbf{n} dS \quad (\text{A6})$$

Therefore, Eq. (A6), which is Eq. (1) in the main text, is equivalent to the expression given by Noca et al. [22] (Sec. 1.1 in their paper). It is emphasized that Eq. (1) can be directly obtained from the incompressible NS equations.

A2 Reformulation of the Force Formula

By neglecting the viscous stress term at the surface Σ , Eq. (2) is

$$\begin{aligned} \mathbf{F} = & \rho \int_{V_f} \mathbf{u} \times \boldsymbol{\omega} dV - \rho \int_{V_f} \frac{\partial \mathbf{u}}{\partial t} dV - \oint_{\Sigma} (p + \rho q^2/2) \mathbf{n} dS \\ & - \rho \oint_{\partial B} (q^2/2) \mathbf{n} dS \end{aligned} \quad (\text{A7})$$

A useful vector identity is $\mathbf{x} \times \nabla \times \mathbf{A} = (N-1)\mathbf{A} + \nabla(\mathbf{x} \cdot \mathbf{A}) - \nabla \cdot (\mathbf{x}\mathbf{A})$, where the spatial dimensionality is defined as $N=2$ for 2-D or 3 for 3-D, \mathbf{x} is the spatial position vector, and \mathbf{A} an arbitrary vector. Setting $\mathbf{A} = \mathbf{u}$ in the previous identity yields a relation between the velocity and the vorticity moment:

$$\mathbf{u} = \frac{1}{k}(\mathbf{x} \times \boldsymbol{\omega}) - \frac{1}{k}[\nabla(\mathbf{x} \cdot \mathbf{u}) - \nabla \cdot (\mathbf{x}\mathbf{u})] \quad (\text{A8})$$

where $k=N-1$ and $N=2, 3$ is the number of spatial dimensionality. By using Eq. (A8), Gauss's theorem, and a vector identity $(\mathbf{x} \cdot \mathbf{A})\mathbf{n} - (\mathbf{x}\mathbf{A}) \cdot \mathbf{n} = \mathbf{x} \times \mathbf{n} \times \mathbf{A}$, the local acceleration term in Eq. (A7) can be expressed as

$$\begin{aligned} -\rho \int_{V_f} \frac{\partial \mathbf{u}}{\partial t} dV = & -\frac{\rho}{k} \int_{V_f} \mathbf{x} \times \frac{\partial \boldsymbol{\omega}}{\partial t} dV + \frac{\rho}{k} \int_{V_f} \frac{\partial}{\partial t} [\nabla(\mathbf{x} \cdot \mathbf{u}) - \nabla \cdot (\mathbf{x}\mathbf{u})] dV \\ = & -\frac{\rho}{k} \int_{V_f} \mathbf{x} \times \frac{\partial \boldsymbol{\omega}}{\partial t} dV + \frac{\rho}{k} \oint_{\Sigma} \mathbf{x} \times \mathbf{n} \times \frac{\partial \mathbf{u}}{\partial t} dS \\ & + \frac{\rho}{k} \oint_{\partial B} \mathbf{x} \times \mathbf{n} \times \frac{\partial \mathbf{u}}{\partial t} dS \end{aligned} \quad (\text{A9})$$

Further, by using the NS equations $\rho \partial \mathbf{u} / \partial t = \rho \mathbf{u} \times \boldsymbol{\omega} - \nabla(p + \rho q^2/2) + \mu \nabla^2 \mathbf{u}$ and an identity given by Noca et al. [22] for a scalar field ϕ ,

$$\oint_S \mathbf{x} \times \mathbf{n} \times (\nabla \phi) dS = -k \oint_S \phi \mathbf{n} dS \quad (\text{A10})$$

the second term in the last line of Eq. (A9) is written as

$$\begin{aligned} \frac{\rho}{k} \oint_{\Sigma} \mathbf{x} \times \mathbf{n} \times \frac{\partial \mathbf{u}}{\partial t} dS \\ = \frac{1}{k} \oint_{\Sigma} \rho \mathbf{x} \times \mathbf{n} \times (\mathbf{u} \times \boldsymbol{\omega}) dS + \oint_{\Sigma} (p + \rho q^2/2) \mathbf{n} dS \\ + \frac{1}{k} \oint_{\Sigma} \mathbf{x} \times \mathbf{n} \times (\mu \nabla^2 \mathbf{u}) dS \end{aligned} \quad (\text{A11})$$

Combining Eqs. (A7), (A9), and (A11) and neglecting the viscous diffusion term on the outer control surface, we have

$$\begin{aligned} \mathbf{F} = & \rho \int_{V_f} \mathbf{u} \times \boldsymbol{\omega} dV - \frac{\rho}{k} \int_{V_f} \mathbf{x} \times \frac{\partial \boldsymbol{\omega}}{\partial t} dV + \frac{\rho}{k} \oint_{\Sigma} \mathbf{x} \times \mathbf{n} \times (\mathbf{u} \times \boldsymbol{\omega}) dS \\ & + \frac{\rho}{k} \oint_{\partial B} \mathbf{x} \times \mathbf{n} \times \frac{\partial \mathbf{u}}{\partial t} dS - \rho \oint_{\partial B} (q^2/2) \mathbf{n} dS \end{aligned} \quad (\text{A12})$$

Eq. (A12) is a reformulated form of Eq. (A7) that is more suitable for comparison with the force expressions given by Wu et al. [24] and Noca et al. [22].

A3 Connection to the Advection Form Force Formula

From Eq. (A6), Wu et al. [24] have derived three equivalent force expressions by using the so-called derivative-moment transformations. One is the advection form expressed as

$$\mathbf{F} = -\rho \int_{V_f} \left(\frac{1}{k} \mathbf{x} \times \frac{\partial \boldsymbol{\omega}}{\partial t} - \mathbf{l} \right) dV + \frac{\rho}{k} \oint_{\partial V_f} \mathbf{x} \times (\mathbf{n} \times \mathbf{l}) dS + \mathbf{F}_B + \mathbf{F}_{\Sigma} \quad (\text{A13})$$

$$\mathbf{F}_B = \frac{1}{k} \oint_{\partial B} \rho \mathbf{x} \times (\mathbf{n} \times \mathbf{a}) dS \quad (\text{A14})$$

$$\mathbf{F}_{\Sigma} = -\frac{\mu}{k} \oint_{\Sigma} \mathbf{x} \times [\mathbf{n} \times (\nabla \times \boldsymbol{\omega})] dS + \mu \oint_{\Sigma} \boldsymbol{\omega} \times \mathbf{n} dS \quad (\text{A15})$$

where V_f is the control volume, $\partial V_f = \partial B + \Sigma$ is the control surface, $k=N-1$, and $\mathbf{l} = \mathbf{u} \times \boldsymbol{\omega}$ is the Lamb vector. Substitution of $\mathbf{a} = D\mathbf{u}/Dt = \partial \mathbf{u} / \partial t + \mathbf{l} + \nabla(q^2/2)$ and Eq. (A10) into Eq. (A14) yields

$$\mathbf{F}_B = \frac{1}{k} \oint_{\partial B} \rho \mathbf{x} \times \left(\mathbf{n} \times \frac{\partial \boldsymbol{\omega}}{\partial t} \right) dS - \frac{1}{k} \oint_{\partial B} \rho \mathbf{x} \times (\mathbf{n} \times \mathbf{l}) dS - \rho \oint_{\partial B} (q^2/2) dS \quad (\text{A16})$$

When the viscous term \mathbf{F}_{Σ} on the outer control surface Σ is neglected, combination of Eqs. (A13), (A14), and (A16) leads to Eq. (A12).

A4 Connection to the Momentum Form Force Formula

In classical hydrodynamics, it is known that the hydrodynamic force is proportional to the rate of change of the vorticity impulse with respect to time [16]. The vorticity impulse formulations have been expended by Wu [17] and Noca et al. [22] in the framework of viscous flow theory. From Eq. (A4), Noca et al. [22] have derived three equivalent force expressions. Noca et al. gave the so-called momentum equation

$$\mathbf{F} = -\frac{d}{dt} \int_{V_f} \mathbf{u} dV + \oint_{\Sigma} \mathbf{n} \cdot \gamma_{\text{mom}} dS - \oint_{\partial B} \mathbf{n} \cdot (\mathbf{u} - \mathbf{U}_B) \mathbf{u} dS \quad (\text{A17})$$

where

$$\begin{aligned} \gamma_{\text{mom}} = & \frac{1}{2} u^2 \mathbf{I} + (\mathbf{U}_{\Sigma} - \mathbf{u}) \mathbf{u} - \frac{1}{k} \mathbf{u} (\mathbf{x} \times \boldsymbol{\omega}) + \frac{1}{k} \boldsymbol{\omega} (\mathbf{x} \times \mathbf{u}) \\ & - \frac{1}{k} \left[\left(\mathbf{x} \cdot \frac{\partial \mathbf{u}}{\partial t} \right) \mathbf{I} - \mathbf{x} \frac{\partial \mathbf{u}}{\partial t} \right] + \frac{1}{k} [\mathbf{x} \cdot (\nabla \cdot \boldsymbol{\tau}) \mathbf{I} - \mathbf{x} (\nabla \cdot \boldsymbol{\tau})] + \boldsymbol{\tau} \end{aligned}$$

\mathbf{I} is the unit tensor, $\boldsymbol{\tau}$ is the viscous stress tensor, and the fluid density is $\rho = 1$. The third term in RHS of Eq. (A17) is zero after the nonslip boundary condition is applied. When the viscous terms on the outer control surface Σ is neglected, Eq. (A17) is reduced to

$$\begin{aligned} \mathbf{F} = & -\frac{d}{dt} \int_{V_f} \mathbf{u} dV + \oint_{\Sigma} \mathbf{n} \cdot \left[\frac{1}{2} u^2 \mathbf{I} - \mathbf{u} \mathbf{u} \right] dS + \oint_{\Sigma} \mathbf{n} \cdot \mathbf{u}_{\Sigma} dS \\ & - \frac{1}{k} \oint_{\Sigma} \mathbf{n} \cdot [\mathbf{u} (\mathbf{x} \times \boldsymbol{\omega}) - \boldsymbol{\omega} (\mathbf{x} \times \mathbf{u})] dS - \frac{1}{k} \oint_{\Sigma} \mathbf{n} \cdot \left[\left(\mathbf{x} \cdot \frac{\partial \mathbf{u}}{\partial t} \right) \mathbf{I} - \mathbf{x} \frac{\partial \mathbf{u}}{\partial t} \right] dS \end{aligned} \quad (\text{A18})$$

By using the following identities:

$$\begin{aligned} \frac{d}{dt} \int_{V_f(t)} \mathbf{u} dV = & \int_{V_f(t)} \frac{D\mathbf{u}}{Dt} dV - \oint_{\partial V_f(t)} \mathbf{u} (\mathbf{u} - \mathbf{u}_{\partial V_f(t)}) \cdot \mathbf{n} dS \\ = & \int_{V_f(t)} \frac{\partial \mathbf{u}}{\partial t} dV - \oint_{\partial V_f} \mathbf{u} (\mathbf{u}_{\partial V_f(t)} \cdot \mathbf{n}) dS \end{aligned} \quad (\text{A19})$$

$$\mathbf{n} \cdot [\mathbf{u}(\mathbf{x} \times \boldsymbol{\omega}) - \boldsymbol{\omega}(\mathbf{x} \times \mathbf{u})] = -\mathbf{x} \times \mathbf{n} \times (\mathbf{u} \times \boldsymbol{\omega}) \quad (A20)$$

$$\mathbf{n} \cdot \left[\left(\mathbf{x} \cdot \frac{\partial \mathbf{u}}{\partial t} \right) \mathbf{I} - \mathbf{x} \frac{\partial \mathbf{u}}{\partial t} \right] = \mathbf{x} \times \mathbf{n} \times \frac{\partial \mathbf{u}}{\partial t} \quad (A21)$$

$$\oint_{\Sigma} \mathbf{n} \cdot \left(\frac{1}{2} u^2 \mathbf{I} - \mathbf{u} \mathbf{u} \right) dS = \int_{V_f} \mathbf{u} \times \boldsymbol{\omega} dV - \oint_{\partial B} \mathbf{n} \cdot \left(\frac{1}{2} u^2 \mathbf{I} - \mathbf{u} \mathbf{u} \right) dS \quad (A22)$$

and Eq. (A11), Eq. (A18) is reduced to

$$\mathbf{F} = - \int_{V_f} \frac{\partial \mathbf{u}}{\partial t} dV + \int_{V_f} \mathbf{u} \times \boldsymbol{\omega} dV - \oint_{\Sigma} (p + q^2/2) \mathbf{n} dS - \oint_{\partial B} (q^2/2) \mathbf{n} dS \quad (A23)$$

Eq. (A23) is the same as Eq. (A7) for $\rho = 1$.

A5 Connection to the Auxiliary Potential Form Force Formula

To extract the pressure force, an auxiliary velocity potential satisfying suitable boundary conditions has been used by several researchers [18–20]. Chang [20] has given the expressions of the pressure force for three unsteady flows, and here one of them is compared with the present force formula as an example. For a body rotating with a angular velocity $\boldsymbol{\Omega} = \boldsymbol{\Omega}(t)$ in a constant stream $\mathbf{c} = -ci$, an expression for the force component is

$$\begin{aligned} F_{\alpha} = \mathbf{F} \cdot \boldsymbol{\alpha} &= \frac{\rho}{c} \oint_{\partial B} \phi \frac{\partial \mathbf{u}}{\partial t} \cdot \mathbf{n} dS - \frac{\rho}{2} \oint_{\partial B} q^2 (\boldsymbol{\alpha} \cdot \mathbf{n}) dS \\ &- \frac{\rho}{c} \int_{V_{\infty}} \mathbf{u} \times \boldsymbol{\omega} \cdot \nabla \phi dV + \frac{\mu}{c} \oint_{\partial B} \mathbf{n} \times \boldsymbol{\omega} \cdot (\nabla \phi) dS + \mu \oint_{\partial B} \mathbf{n} \times \boldsymbol{\omega} \cdot \boldsymbol{\alpha} dS \end{aligned} \quad (A24)$$

The auxiliary potential ϕ satisfies the Laplace equation $\nabla^2 \phi = 0$ with the boundary condition $\nabla \phi \cdot \mathbf{n} = -c\boldsymbol{\alpha} \cdot \mathbf{n}$ on the body surface and the far-field condition $\phi|_{r \rightarrow \infty} = 0$ in a body-fixed frame ($\boldsymbol{\alpha}, \boldsymbol{\beta}, \boldsymbol{\gamma}$).

Because $\boldsymbol{\omega} = 0$ in the uniform far-field flow, Eq. (A24) can be written as

$$\begin{aligned} F_{\alpha} &= \frac{\rho}{c} \oint_{\partial B} \phi \frac{\partial \mathbf{u}}{\partial t} \cdot \mathbf{n} dS - \frac{\rho}{2} \oint_{\partial B} q^2 (\boldsymbol{\alpha} \cdot \mathbf{n}) dS - \frac{\rho}{c} \int_{V_{\infty}} \mathbf{u} \times \boldsymbol{\omega} \cdot \nabla \phi dV \\ &+ \mu \oint_{\partial B + \Sigma_{\infty}} \mathbf{n} \times \boldsymbol{\omega} \cdot \left(\frac{\nabla \phi}{c} + \boldsymbol{\alpha} \right) dS \\ &= \frac{\rho}{c} \oint_{\partial B} \phi \frac{\partial \mathbf{u}}{\partial t} \cdot \mathbf{n} dS - \frac{\rho}{2} \oint_{\partial B} q^2 (\boldsymbol{\alpha} \cdot \mathbf{n}) dS - \frac{\rho}{c} \int_{V_{\infty}} \mathbf{u} \times \boldsymbol{\omega} \cdot \nabla \phi dV \\ &+ \mu \int_{V_{\infty}} (\nabla \times \boldsymbol{\omega}) \cdot \left(\frac{\nabla \phi}{c} + \boldsymbol{\alpha} \right) dS \end{aligned} \quad (A25)$$

where Σ_{∞} is the outer control surface at $r \rightarrow \infty$. By using the incompressible NS equations $\rho \partial \mathbf{u} / \partial t - \rho \mathbf{u} \times \boldsymbol{\omega} + \nabla(\rho q^2/2) = -\nabla p - \mu \nabla \times \boldsymbol{\omega}$, Eq. (A25) becomes

$$\begin{aligned} F_{\alpha} &= \rho \int_{V_{\infty}} (\mathbf{u} \times \boldsymbol{\omega}) \cdot \boldsymbol{\alpha} dV - \rho \int_{V_{\infty}} \frac{\partial \mathbf{u}}{\partial t} \cdot \boldsymbol{\alpha} dV - \rho \int_{V_{\infty}} \frac{\partial \mathbf{u}}{\partial t} \cdot \frac{\nabla \phi}{c} dV \\ &- \int_{V_{\infty}} \nabla P \cdot \left(\frac{\nabla \phi}{c} + \boldsymbol{\alpha} \right) dV + \frac{\rho}{c} \oint_{\partial B} \phi \frac{\partial \mathbf{u}}{\partial t} \cdot \mathbf{n} dS - \frac{\rho}{2} \oint_{\partial B} q^2 (\boldsymbol{\alpha} \cdot \mathbf{n}) dS \end{aligned} \quad (A26)$$

where $P = p + \rho q^2/2$ is the total pressure. The fourth term in RHS of Eq. (A26) can be expressed in the surface integral

$$\begin{aligned} - \int_{V_{\infty}} \nabla P \cdot \left(\frac{\nabla \phi}{c} + \boldsymbol{\alpha} \right) dV &= - \oint_{\partial B} P \mathbf{n} \cdot \left(\frac{\nabla \phi}{c} + \boldsymbol{\alpha} \right) dS \\ &- \oint_{\Sigma_{\infty}} P \mathbf{n} \cdot \left(\frac{\nabla \phi}{c} + \boldsymbol{\alpha} \right) dS \end{aligned} \quad (A27)$$

On the body surface, because the boundary condition for ϕ is $\nabla \phi \cdot \mathbf{n} = -c\boldsymbol{\alpha} \cdot \mathbf{n}$, the surface integral on ∂B in Eq. (A27) vanishes. Further, because $\nabla \phi \sim r^{-3}$ decays in 3-D and $\nabla \phi \sim r^{-2}$ in 2-D flow in the far-field flow, Eq. (A27) becomes

$$- \int_{V_{\infty}} \nabla P \cdot \left(\frac{\nabla \phi}{c} + \boldsymbol{\alpha} \right) dV = - \oint_{\Sigma_{\infty}} P \mathbf{n} \cdot \boldsymbol{\alpha} dS \quad (A28)$$

Similarly, the third term in RHS of Eq. (A26) can be expressed in the surface integral

$$-\rho \int_{V_{\infty}} \frac{\partial \mathbf{u}}{\partial t} \cdot \frac{\nabla \phi}{c} dV = -\rho \oint_{\partial B} \frac{\phi \partial \mathbf{u}}{c \partial t} \cdot \mathbf{n} dS - \rho \oint_{\Sigma_{\infty}} \frac{\phi \partial \mathbf{u}}{c \partial t} \cdot \mathbf{n} dS \quad (A29)$$

The first term on the RHS of Eq. (A29) cancels with the fifth term on the RHS of Eq. (A26). In the constant uniform far-field flow where $\partial \mathbf{u} / \partial t = 0$ and $\phi|_{r \rightarrow \infty} = 0$, the surface integral on Σ_{∞} in Eq. (A29) vanishes. Therefore, after the remaining terms in Eq. (A26) are retained, we have

$$\begin{aligned} F_{\alpha} &= \rho \int_{V_{\infty}} (\mathbf{u} \times \boldsymbol{\omega}) \cdot \boldsymbol{\alpha} dV - \rho \int_{V_{\infty}} \frac{\partial \mathbf{u}}{\partial t} \cdot \boldsymbol{\alpha} dV \\ &- \oint_{\Sigma_{\infty}} P \mathbf{n} \cdot \boldsymbol{\alpha} dS - \frac{\rho}{2} \oint_{\partial B} q^2 (\boldsymbol{\alpha} \cdot \mathbf{n}) dS \end{aligned} \quad (A30)$$

The force components $F_{\beta} = \mathbf{F} \cdot \boldsymbol{\beta}$ and $F_{\gamma} = \mathbf{F} \cdot \boldsymbol{\gamma}$ have the same form as Eq. (A30). Therefore, we have

$$\mathbf{F} = \rho \int_{V_{\infty}} \mathbf{u} \times \boldsymbol{\omega} dV - \rho \int_{V_{\infty}} \frac{\partial \mathbf{u}}{\partial t} dV - \oint_{\Sigma_{\infty}} P \mathbf{n} dS - \rho \oint_{\partial B} (q^2/2) \mathbf{n} dS \quad (A31)$$

which is exactly the same as Eq. (A7).

Appendix B: Drag

Although the focus of this work is on the lift problem, it is worthwhile to examine the drag problem. The force in the freestream direction (drag/thrust) on a body is given by

$$\begin{aligned} F_x = \mathbf{i} \cdot \mathbf{F} &= \underbrace{-\rho i \cdot \int_{V_f} \frac{\partial \mathbf{u}}{\partial t} dV}_{A} + \underbrace{\rho i \cdot \int_{V_f} \mathbf{u} \times \boldsymbol{\omega} dV}_{B} - \underbrace{\frac{\rho}{k} i \cdot \oint_{\Sigma} \mathbf{x} \times \mathbf{n} \times \mathbf{v}_p dS}_{C} \\ &+ \underbrace{i \cdot \oint_{\Sigma} \mathbf{n} \cdot \tau dS}_{D} - \underbrace{i \cdot \oint_{\partial B} \rho \frac{q^2}{2} \mathbf{n} dS}_{E} \end{aligned} \quad (B1)$$

where \mathbf{i} is the unit vector parallel to the freestream, $\mathbf{v}_p = \partial \mathbf{u} / \partial t - \mathbf{u} \times \boldsymbol{\omega} - \nu \nabla^2 \mathbf{u}$, and the number of the dimensionality is defined as $k = N - 1 = 2$ for 3-D and $k = N - 1 = 1$ for 2-D. The terms A and E together in Eq. (B1) are the contribution of the acceleration projected on the freestream direction, and in the inviscid irrotational flow, they represent the added-mass drag. The term B is the contribution of the vortex force that physically contains the induced drag and the thrust generated by a flapping wing. The term C is the projected total pressure term in Eq. (2), which is expressed in the terms related to the velocity field by using a surface integral relation given by Noca et al. [22]. In contrast to the lift problem, for a sufficiently large rectangular domain, the total pressure term (the term C) in Eq. (B1) cannot be neglected. In fact, it can be expressed by an integral of $\rho(q_{\infty}^2 - q_1^2)/2 + (p_{\infty} - p_1)$ over a Trefftz plane S_1 , where p_1 and q_1 are the static and dynamic pressures on S_1 , respectively. Physically, the term C represents the parasite drag. For a sufficiently large control surface where flow can be considered to be

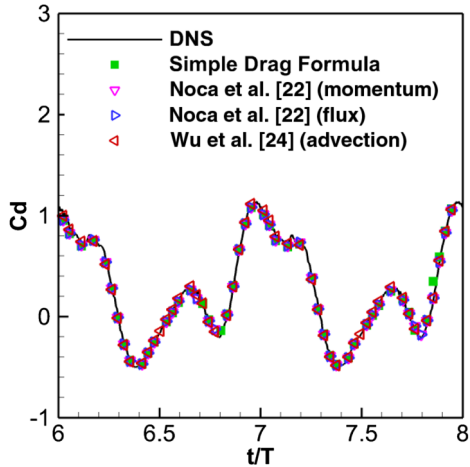


Fig. B1 Time histories of the drag coefficient of the flapping rectangular wing calculated by using the different drag formulas.

inviscid, the term D can be neglected, and the term E is small for a thin wing. Therefore, Eq. (B1), in which only the three major terms remain, is called “the simple drag formula” for convenience. Indeed, the calculated drag coefficients by using the simple drag formula are consistent with DNS for a flapping flat plate and a flapping rectangular wing [26]. Here, the dominant terms in Eq. (B1) in the drag calculations of the flapping rectangular wing as an example are identified in comparison with those in the force formulas of Noca et al. [22] and Wu et al. [24].

The drag coefficients of the flapping rectangular wing are calculated by using the different drag formulas. Figure B1 indicates

that all the different drag formulas give drag coefficients that are consistent with DNS. The label “simple drag formula” indicates the drag coefficients calculated by using Eq. (B1), and the others labels in the figures in this appendix have the same meanings as those in Sec. IV. However, the difference between the drag formulas is the number of the dominant terms needed to recover the history of the unsteady drag. Figure B2 shows the contributions of all the terms in the four drag formulas to the drag coefficient. Equation (B1) has two dominant terms (B and C), and the sum of the other terms (A , D , and E) is much smaller (A , D , and E), as shown in Fig. B2a. The drag coefficient is mainly contributed by the vortex force (the term B) and the parasite drag term (the term C) in Eq. (B1). It is noted that the term A , which represents the contribution from the local fluid acceleration, is small in this case, where the flapping motion is restricted in the vertical direction. This term could become a dominant term when the plate has streamwise acceleration.

In contrast, as shown in Figs. B2b and B2c, both the momentum equation and the flux equation [Eqs. (4) and (5)] given by Noca et al. [22] have four dominant terms. All these dominant terms relate to the contributions from the fluxes of the momentum, vorticity moment, and velocity moment across the outer control surface. It is noted that the acceleration term (the term A) in the momentum equation does not contribute much to the drag in this case, although its contribution to the unsteady lift is significant. However, it could be significant when the wing has streamwise acceleration. As shown in Fig. B2d, there are three dominant terms [A , B , and C in Eq. (6)] in the advection form of the force formula given by Wu et al. [24]. In Eq. (6), the term B is the contribution from the vortex force, and the terms A and C together contribute to the parasite drag plus the acceleration term projected onto the freestream direction. It is observed that the terms A , B , and C are also the dominant terms contributing the lift.

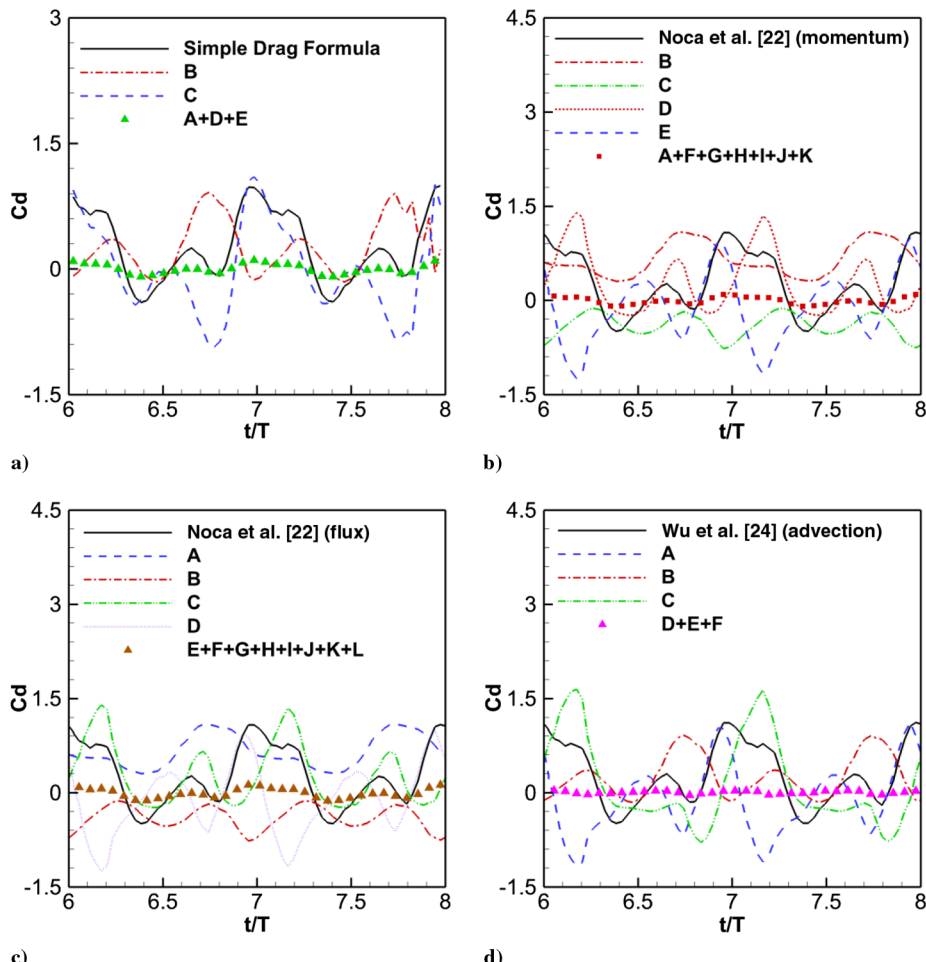


Fig. B2 Contributions of the terms to the drag coefficient of the flapping rectangular wing in the different drag formulas.

Acknowledgments

This work was supported by the National Natural Science Foundation of China under project numbers 10872201, 11232011, 11302238, and 11372331, and the National Basic Research Program of China (973 Program) under project number 2013CB834100 (nonlinear science). We would like to acknowledge the support from the National Supercomputer Center in Tianjin. We would like to thank Jiezhli Wu of Peking University and the University of Tennessee Space Institute for his detailed constructive comments. Tianshu Liu would like to acknowledge the hospitality received at State Key Laboratory of Nonlinear Mechanics during his visit where he accomplished this work. The simulations were performed on TianHe-1.

References

- [1] Platzer, M. F., Jones, K. D., Young, J., and Lai, J. C. S., "Flapping Wing Aerodynamics: Progress and Challenges," *AIAA Journal*, Vol. 46, No. 9, 2008, pp. 2136–2149.
doi:10.2514/1.29263
- [2] Shyy, W., Lian, Y., Tang, J., Viieru, D., and Liu, H., *Aerodynamics of Low Reynolds Number Flyers*, Cambridge Univ. Press, Cambridge, England, U.K., 2008, pp. 101–158.
- [3] Liu, H., Nakata, T., Gao, N., Maeda, M., Aono, H., and Shyy, W., "Micro Air Vehicle-Motivated Computational Biomechanics in Bio-Flights: Aerodynamics, Flight Dynamics and Maneuvering Stability," *Acta Mechanica Sinica*, Vol. 26, No. 6, 2010, pp. 863–879.
doi:10.1007/s10409-010-0389-5
- [4] Wu, J. H., Zhang, Y. L., and Sun, M., "Hovering of Model Insects: Simulation by Coupling Equations of Motion with Navier–Stokes Equations," *Journal of Experimental Biology*, Vol. 212, No. 20, 2009, pp. 3313–3329.
doi:10.1242/jeb.030494
- [5] Spedding, G. R., Rosen, M., and Hedenstrom, A., "A Family of Vortex Wakes Generated by a Thrush Nightingale in Free Flight in a Wind Tunnel Over Its Entire Natural Range of Flight Speeds," *Journal of Experimental Biology*, Vol. 206, No. 14, 2003, pp. 2313–2344.
doi:10.1242/jeb.00423
- [6] Hedenstrom, A., Johansson, L. C., Wolf, M., von Busse, R., Winter, Y., and Spedding, G. R., "Bat Flight Generates Complex Aerodynamic Tracks," *Science*, Vol. 316, No. 5826, 2007, pp. 894–897.
doi:10.1126/science.1142281
- [7] Hubel, T. Y., Hristov, N. I., Swartz, S. M., and Breuer, K. S., "Time-Resolved Wake Structure and Kinematics of Bat Flight," *Experiments in Fluids*, Vol. 46, No. 5, 2009, pp. 933–943.
doi:10.1007/s00348-009-0624-7
- [8] Yu, M., Wang, Z. J., and Hu, H., "Formation of Bifurcated Wakes Behind Finite Span Flapping Wings," *AIAA Journal*, Vol. 51, No. 8, 2013, pp. 2040–2044.
doi:10.2514/1.J052300
- [9] Hu, H., Clemons, L., and Igarashi, H., "An Experimental Study of the Unsteady Vortex Structures in the Wake of a Root-Fixed Flapping Wing," *Experiments in Fluids*, Vol. 51, No. 2, 2011, pp. 347–359.
doi:10.1007/s00348-011-1052-z
- [10] Zheng, Z. C., and Wei, Z., "Study of Mechanisms and Factors that Influence the Formation of Vortical Wake of a Heaving Airfoil," *Physics of Fluids*, Vol. 24, No. 10, 2012, Paper 103601.
doi:10.1063/1.4760258
- [11] Rayner, J. M. V., "Vortex Theory of Animal Flight. Part 1. Vortex Wake of a Hovering Animal," *Journal of Fluid Mechanics*, Vol. 91, No. 4, April 1979, pp. 697–730.
doi:10.1017/S0022112079000410
- [12] Rayner, J. M. V., "Vortex Theory of Animal Flight. Part 2. Forward Flight of Birds," *Journal of Fluid Mechanics*, Vol. 91, No. 4, 1979, pp. 731–763.
doi:10.1017/S0022112079000422
- [13] Watts, P., Mitchell, E. J., and Swartz, S. M., "A Computational Model for Estimating the Mechanics of Horizontal Flapping Flight in Bats: Model Description and Validation," *Journal of Experimental Biology*, Vol. 204, No. 16, 2001, pp. 2873–2898.
- [14] Sane, S. P., "The Aerodynamics of Insect Flight," *Journal of Experimental Biology*, Vol. 206, No. 23, 2003, pp. 4191–4208.
doi:10.1242/jeb.00663
- [15] Ansari, S. A., Zbikowski, R., and Knowles, K., "Aerodynamic Modelling of Insect-Like Flapping Flight for Micro Air Vehicles," *Progress in Aerospace Sciences*, Vol. 42, No. 2, 2006, pp. 129–172.
doi:10.1016/j.paerosci.2006.07.001
- [16] Saffman, P. G., *Vortex Dynamics*, Cambridge Univ. Press, Cambridge, England, U.K., 1992, Chaps. 3–4.
- [17] Wu, J. C., "Theory for Aerodynamic Force and Moment in Viscous Flows," *AIAA Journal*, Vol. 19, No. 4, 1981, pp. 432–441.
doi:10.2514/3.50966
- [18] Quartapelle, L., and Napolitano, M., "Force and Moment in Incompressible Flows," *AIAA Journal*, Vol. 21, No. 6, 1983, pp. 911–912.
doi:10.2514/3.8171
- [19] Howe, M. S., "On Unsteady Surface Forces, and Sound Produced by the Normal Chopping of a Rectilinear Vortex," *Journal of Fluid Mechanics*, Vol. 206, No. 9, 1989, pp. 131–153.
doi:10.1017/S0022112089002259
- [20] Chang, C.-C., "Potential Flow and Forces for Incompressible Viscous Flow," *Proceedings of the Royal Society of London. Series A: Mathematical and Physical Sciences*, Vol. 437, No. 1901, 1992, pp. 517–525.
doi:10.1098/rspa.1992.0077
- [21] Wu, J. Z., and Wu, J. M., "Vorticity Dynamics on Boundaries," *Advances in Applied Mechanics*, Vol. 32, Academic Press, San Diego, CA, 1996, pp. 119–275.
- [22] Noca, F., Shiels, D., and Jeon, D., "A Comparison of Methods for Evaluating Time-Dependent Fluid Dynamic Forces on Bodies, Using Only Velocity Fields and Their Derivatives," *Journal of Fluids and Structures*, Vol. 13, No. 5, 1999, pp. 551–578.
doi:10.1006/jfls.1999.0219
- [23] Wu, J.-Z., Pan, Z.-L., and Lu, X.-Y., "Unsteady Fluid-Dynamic Force Solely in Terms of Control-Surface Integral," *Physics of Fluids*, Vol. 17, No. 9, 2005, Paper 098102.
doi:10.1063/1.2055528
- [24] Wu, J. Z., Ma, H. Y., and Zhou, M. D., *Vorticity and Vortex Dynamics*, Springer, Berlin, 2006, Chap. 11.
- [25] Marongiu, C., and Tognaccini, R., "Far-Field Analysis of the Aerodynamic Force by Lamb Vector Integrals," *AIAA Journal*, Vol. 48, No. 11, 2010, pp. 2543–2555.
doi:10.2514/1.J050326
- [26] Wang, S. Z., Zhang, X., He, G. W., and Liu, T. S., "A Lift Formula Applied to Low-Reynolds-Number Unsteady Flows," *Physics of Fluids*, Vol. 25, No. 9, 2013, Paper 093605.
doi:10.1063/1.4821520
- [27] von Kármán, T., and Sears, W. R., "Airfoil Theory for Non-Uniform Motion," *Journal of Aeronautical Sciences*, Vol. 5, No. 10, 1938, pp. 379–390.
doi:10.2514/8.674
- [28] Baik, Y. S., Bernal, L., Shyy, W., and Ol, M., "Unsteady Force Generation and Vortex Dynamics of Pitching and Flat Plates at Low Reynolds Number," *49th AIAA Aerospace Sciences Meeting*, AIAA Paper 2011-0220, Jan. 2011.
- [29] Wang, S. Z., and Zhang, X., "An Immersed Boundary Method Based on Discrete Stream Function Formulation for Two- and Three-Dimensional Incompressible Flows," *Journal of Computational Physics*, Vol. 230, No. 9, 2011, pp. 3479–3499.
doi:10.1016/j.jcp.2011.01.045
- [30] Chang, W., Giraldo, F., and Perot, B., "Analysis of an Exact Fractional Step Method," *Journal of Computational Physics*, Vol. 180, No. 1, 2002, pp. 183–199.
doi:10.1006/jcph.2002.7087
- [31] Peskin, C. S., "The Immersed Boundary Method," *Acta Numerica*, Vol. 11, Jan. 2002, pp. 479–517.
doi:10.1017/S0962492902000077
- [32] Wang, S., He, G., Zhang, X., and Liu, T., "Lift Enhancement by Dynamically Changing Wingspan in Forward Flapping Flight," *Physics of Fluids*, Vol. 26, No. 6, 2014, Paper 061903.
doi:10.1063/1.4884130

Z. Rusak
Associate Editor